Evolutionarily Stable Strategy Carbon Allocation to Foliage, Wood, and Fine Roots in Trees Competing for Light and Nitrogen: An Analytically Tractable, Individual-Based Model and Quantitative Comparisons to Data

Ray Dybzinski,[1,*] Caroline Farrior,[1] Adam Wolf,[2] Peter B. Reich,[3] and Stephen W. Pacala[1]

1. Department of Ecology and Evolutionary Biology, Princeton University, Princeton, New Jersey 08544; 2. Department of Global Ecology, Carnegie Institution for Science, Stanford, California 94305; 3. Department of Forest Resources, University of Minnesota, St. Paul, Minnesota 55108

Submitted April 28, 2010; Accepted October 26, 2010; Electronically published January 12, 2011

Online enhancements: appendixes.

ABSTRACT: We present a model that scales from the physiological and structural traits of individual trees competing for light and nitrogen across a gradient of soil nitrogen to their community-level consequences. The model predicts the most competitive (i.e., the evolutionarily stable strategy [ESS]) allocations to foliage, wood, and fine roots for canopy and understory stages of trees growing in old-growth forests. The ESS allocations, revealed as analytical functions of commonly measured physiological parameters, depend not on simple root-shoot relations but rather on diminishing returns of carbon investment that ensure any alternate strategy will underperform an ESS in monoculture because of the competitive environment that the ESS creates. As such, ESS allocations do not maximize nitrogen-limited growth rates in monoculture, highlighting the underappreciated idea that the most competitive strategy is not necessarily the "best," but rather that which creates conditions in which all others are "worse." Data from 152 stands support the model's surprising prediction that the dominant structural trade-off is between fine roots and wood, not foliage, suggesting the "root-shoot" trade-off is more precisely a "root-stem" trade-off for long-lived trees. Assuming other resources are abundant, the model predicts that forests are limited by both nitrogen and light, or nearly so.

Keywords: perfect plasticity approximation (PPA), FLUXNET, optimal, optimization, forest dynamics, height-structured competition.

Introduction

Just as the physical properties of a moving fluid depend on the characteristics and interactions of individual atoms, the dynamics of the world's forests depend on the characteristics and interactions of individual trees. In the physical sciences, the Navier-Stokes equations successfully scale up processes at the level of atoms to those of fluids. In principle, ecologists should be able to scale up the traits, interactions, and biotic and abiotic environments of individual trees to the population, community, and ecosystem properties of forests (Purves and Pacala 2008). However, a tractable path from the idiosyncrasies of individual trees to the repeatable properties of forests is not obvious.

Building on a body of theoretical and empirical literature (von Foerster 1959; Mitchell 1975; Metz and Diekmann 1986; DeAngelis et al. 1993; Umeki 1995; Pacala et al. 1996; De Roos and Persson 2001), recent advances have produced the "perfect plasticity approximation" (PPA; Strigul et al. 2008). The PPA uses the fact that light competition regulates forest canopies in a way that is effectively independent of the spatial arrangement of individuals to scale from the "mean field" vital rates of individual trees to emergent properties at the level of forests using a physiologically structured population model (Strigul et al. 2008). It generates analyzable "macroscopic equations" that can be used to understand and predict forest structure and dynamics in much the same way that Lotka-Volterra equations can be used to understand generalized species interactions. But unlike the entirely phenomenological Lotka-Volterra equations, the PPA is based on a mechanistic treatment of height-structured competition using quantifiable, individual plant vital rates and, as such, is capable of quantitative predictions that can be tested with available data. Strigul et al. (2008) showed that the PPA captures essential dynamics of forest simulators, which themselves have been shown to capture essential properties of real forests (Di Lucca 1998). Purves et al. (2008) showed that a version of the PPA parameterized with empirically derived vital rates of the dominant tree species in the Great

* Corresponding author; e-mail: rdybzins@princeton.edu.

Am. Nat. 2011. Vol. 177, pp. 153–166.
0003-0147/2011/17702-52118$15.00.
DOI: 10.1086/657992

Lakes states of the United States successfully predicted aspects of forest composition and dynamics over a century of succession.

Here, we characterize the interactions of individual trees using stoichiometrically and physiologically based (i.e., as mechanistic in concept as possible and based on measurable parameters wherever possible) formulations for nitrogen and light competition that, together with quantitative allometric equations, lead to individual growth rates. With these individual growth rates, we use the macroscopic equations of the PPA to scale up to the community level. With community-level equations, we use adaptive dynamics (Geritz et al. 1998; Falster and Westoby 2003; McGill and Brown 2007) to determine the most competitive allocational strategies (i.e., evolutionarily stable strategies [ESSs]), which are not necessarily the growth-maximizing strategies in monoculture. While there are many models of plant competition for nitrogen and light (e.g., Tilman 1988; Reynolds and Pacala 1993; Rees and Bergelson 1997; Friedlingstein et al. 1999), we believe this is the first that is both analytically tractable and capable of accurate quantitative predictions of forestry data. Moreover, its ability to be modified for other types of vegetation and other types of interactions is promising.

Following Tilman (1988), we focus our ESS analysis on predictions of foliage, wood, and fine root allocation in stable-size-distribution (i.e., old-growth) stands across a nitrogen availability gradient. Although we believe that trees also shift both physiology and morphology of foliage, wood, and fine roots to remain competitive across gradients, we restrict the present analysis to shifts in allocation only, holding physiological and morphological parameters constant among strategies. This allows us to evaluate how far we can go in predicting forest processes based solely on understanding ESSs for allocation. We use parameter values for temperate deciduous broadleaf forests and remain uncommitted as to whether shifts in strategy across the gradient represent species replacement or the plastic responses of a single species. The truth is likely somewhere in between and is a worthy subject of future research. In contrast to most untested ESS models of plant dynamics (Falster and Westoby 2003), we tested the model's predictions against empirical allocational patterns from 152 primarily temperate deciduous and evergreen stands from the FLUXNET database (Luyssaert et al. 2007) and Santantonio (1989).

The organization of what follows presents the reader with options depending on his or her interest in the technical details of the model and results. The first section, "Nontechnical Model and Results Summary," provides a heuristic overview that, together with "Model Predictions Compared to Empirical NPP Data," will allow the reader to move on to the "Discussion." The second and third sections, "Quantitative Description of the Model" and "Analytical and Quantitative Results," minimally define the model and report its results in mathematical terms. Appendix G in the online edition of the *American Naturalist* is carefully prepared to stand alone and includes a full model derivation and description, the technical derivation of the results, and additional nontechnical explanations and biological justifications. Table 1 lists all model symbols and parameters, allowing the reader to move between sections without complication. Figure 1 provides a conceptual depiction of the model.

Nontechnical Model and Results Summary

Our model is individual based. Individuals possess strategies for allocating carbon (photosynthate) to foliage, wood, and fine roots. Individuals acquire nitrogen via belowground competition. Nitrogen uptake is proportional to fine root mass, and so individuals with relatively greater fine root mass acquire a greater relative share of the available nitrogen. A close approximation to a full nitrogen cycling model shows that the net mineralization rate is approximately constant and outside of plant control under the conditions considered here. Belowground competition is modeled as mean field, a reasonable approximation of root systems that are extensively commingled. Individuals acquire carbon via photosynthesis, which depends on light availability. Self-shading potentially diminishes the carbon fixed by leaves situated lower in a crown, and canopy individuals shade understory individuals. Carbon allocation to foliage is stoichiometrically constrained by nitrogen uptake, such that individuals cannot build more foliage than they have the nitrogen to support.

We place individuals within a forest stand that is of effectively infinite extent. We restrict our analysis to conditions in which the canopy is closed. The PPA allows us to separate an individual's life into two stages: an understory stage during which its topmost leaves are shaded by the canopy individuals above it and, assuming it survives, a canopy stage during which its topmost leaves receive full sun. Individuals transition from the understory to the canopy stage when they grow to height $\tilde{Z}_r$, whereupon their light environment changes instantaneously and discontinuously (derived as an approximation to a more realistic gradual transition; see app. B in the online edition of the *American Naturalist*). Individuals are subject to a constant mortality rate in the understory and a (lesser) constant mortality rate in the canopy. We assume that only individuals in the canopy stage reproduce.

To find the most competitive allocation strategy, we effectively analyze a series of invasions. We compose the stand of a resident type. Individuals of the resident type all employ the same allocational strategy in the understory

Table 1: Traits subject to evolutionarily stable strategy analysis, parameters, and subscripts

Symbol	Value	Units	Description
$L_{X,x}$	Any (but see eq. [2])	$m^2\ m^{-2}$	Leaf area index; one-sided area of leaves per ground surface area of an individual, proportional to carbon allocation to foliage; constrained by nitrogen stoichiometry (eq. [2])
$G_{X,x}$	Any	cm $year^{-1}$	Stem diameter growth rate, proportional to carbon allocation to wood
$R_{X,x}$	Any	$g_{carbon}\ m^{-2}$	Live fine root mass per crown area; proportional to carbon allocation to fine roots
Nitrogen:			
N_{avail}	Any	$g_N\ m^{-2}\ year^{-1}$	Available nitrogen per area
$N_{X,x}$	Any	$g_N\ m^{-2}$	Nitrogen uptake of an individual per crown area
ρ	.5	None	Fraction of total plant nitrogen uptake allocated to leaves
δ_L	1.595	$g_N\ m^{-2}$	Nitrogen per unit leaf area
f	.5	None	Fraction of nitrogen lost from senesced foliage
γ_L	1	$year^{-1}$	Foliage turnover
Light and photosynthesis:			
I_X^0	0–1	PAR PAR_0^{-1}	Light level of the highest leaf layer
$I_{X,x}^{bottom}$	0–1	PAR PAR_0^{-1}	Light level of the lowest leaf layer
$\tilde{I}$	.33	PAR PAR_0^{-1}	Light level at which photosynthesis is balanced between light limited and light saturated; equal to $(A_{max} + q)/\phi$
A_{max}	9.9×10^{-5}	$g_{carbon}\ LAI^{-1}\ m^{-2}\ s^{-1}$	Maximum net carbon assimilation rate (see fig. 2)
q	9.9×10^{-6}	$g_{carbon}\ LAI^{-1}\ m^{-2}\ s^{-1}$	Dark respiration rate (see fig. 2)
Φ	3.27×10^{-4}	$g_{carbon}\ LAI^{-1}\ m^{-2}\ s^{-1}\ PAR^{-1}\ PAR_0$	Quantum yield of light-limited net photosynthesis (see fig. 2)
s	2.26×10^6	s $year^{-1}$	Scale conversion between measured (s^{-1}) and yearly net photosynthesis
k	.5	LAI^{-1}	Light extinction coefficient per crown depth
ζ	.75	None	Scales k and $L_{C,r}$ in Beer's law light extinction to calculate I_U^0
Carbon:			
$E_{X,x}$	Any	$g_{carbon}\ m^{-2}\ year^{-1}$	Carbon fixed per projected crown area, net after leaf maintenance respiration
M	28	$g_{carbon}\ LAI^{-1}\ m^{-2}$	Leaf carbon per area
κ_L	.25	None	Foliage construction respiration, expressed as a fraction of leaf carbon
γ_R	.3	$year^{-1}$	Fine root turnover
κ_R	.25	None	Fine root construction respiration, expressed as a fraction of fine root carbon
Ω	.35	$g_{carbon}\ g_{carbon}^{-1}\ year^{-1}$	Fine root respiration rate
ω_C	34.6, 0	$g_{carbon}\ m^{-2}\ year^{-1}$	Carbon cost of producing seeds; 0 for understory individuals
Λ	.78	None	Fraction aboveground of the carbon allocated to wood
Perfect plasticity approximation:			
α	.1	$m^{2/\theta}\ cm^{-1}$	Power law coefficient relating D to A
θ	1.4	None	Power law exponent relating D to A
a	81.5	$g_{carbon}\ cm^{-(\theta+1)}$	Power law coefficient relating D to B
W_x	Any	individuals	Fitness or lifetime reproductive success of strategy x
$\tilde{D}_r$	Any	cm	Stem diameter of shortest cohort in the canopy of a monoculture
$\tilde{Z}_r$	Any	m	Height of shortest cohort in the canopy of a monoculture
μ_X	.013, .038	$year^{-1}$	Mortality rate, canopy and understory, respectively
F	.01	individuals $m^{-2}\ year^{-1}$	Germinants produced per unit canopy area per time

Note: Sources and derivations for values are in appendix E in the online edition of the *American Naturalist*. Subscripts and superscripts: r = variables for resident strategies; m = variables for invading strategies; x = a "placeholder" for variables that can take either an r or an m; C = variables for canopy individuals; U = variables for understory individuals; X = a "placeholder" for variables that can take either C or U; asterisk = variables for evolutionarily stable strategies; sat = variables calculated assuming saturating nitrogen uptake. PAR = photosynthetically active radiation; LAI = leaf area per ground area of an individual.

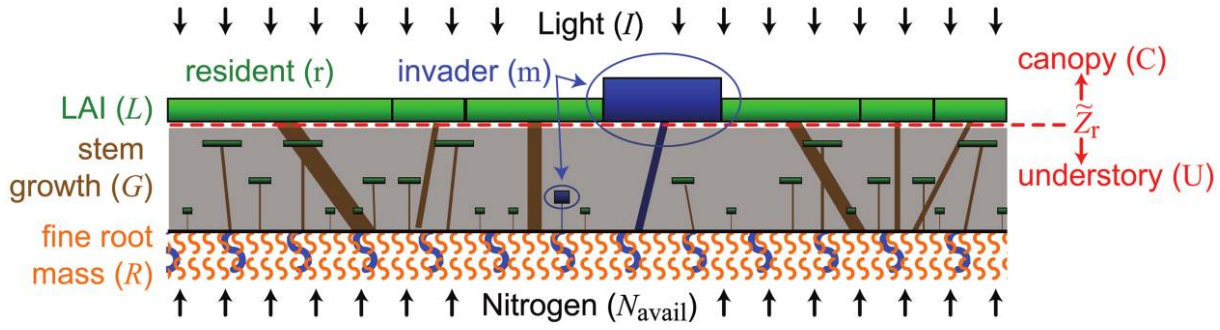

Figure 1: Conceptual figure. Horizontal rectangles are tree crowns with height proportional to leaf area per ground area of an individual (LAI). Vertical or slanted rectangles are stems. Orange "squiggles" are fine root mass, shown without connection to any individuals to reflect the assumption that nitrogen competition is mean field. Here, an invader type is shown that has a higher investment in fine roots per unit crown area (*larger blue squiggles*). Light is reduced due to self-shading (gradient within crowns) and transmittance through the canopy (*gray "shade" in understory*). Parenthetical symbols reflect their use in the model.

stage and the same allocational strategy in the canopy stage, that is, the allocational strategies between the two stages may differ but are uniform within a stage. We solve the system for dynamic equilibrium, such that the transition height from understory to canopy, $\tilde{Z}_r$, and the size distribution of the stand do not change with time.

We then add invader types to the resident stand, where the invader types differ from the resident in their allocational strategies in the understory, the canopy, or both. Importantly, if the invader's fine root allocation is greater than that of the resident, it will be able to acquire relatively more nitrogen, allowing it to build greater stoichiometrically constrained foliage. If the invader's fine root allocation is less than that of the resident, the opposite is true. Whether an invader will grow faster than the resident (i.e., allocate more carbon to wood) depends on the relative carbon costs and benefits of its fine root and foliage allocations in the environment set by the resident.

The population density of the invader type is assumed to be negligible, such that the resident's allocation strategy affects the nitrogen and light availability of the invader but not the other way around. An invader will be successful if its population is expected to increase from low density. In a given habitat (here defined by nitrogen availability), we test all possible resident types against all possible invader types and deem the resident type that resists invasion by all invader types the evolutionarily stable strategy, that is, the most competitive strategy for that habitat.

Our model analysis reveals five important results. (1) In nitrogen-limited habitats, ESS allocation to foliage increases with increasing soil nitrogen availability. In nitrogen-saturated habitats, ESS allocation to foliage is independent of soil nitrogen availability and is determined solely by light availability, such that the lowest, most-shaded leaves in a crown fix just enough carbon to balance the costs of their respiration and construction. (2) Up to the point of nitrogen saturation, ESS allocation to fine roots decreases with increasing soil nitrogen availability. For a particular soil nitrogen availability, ESS allocation to fine roots ensures that invaders with greater fine root allocation will fail to cover their cost with the additional foliage they are able to build. (3) Up to the point of nitrogen saturation, ESS allocation to wood generates increasing stem diameter growth rates with increasing soil nitrogen availability. (4) Closed-canopy forests are necessarily dual limited by nitrogen and light, or nearly so. Habitats with low soil nitrogen availability (i.e., that might be solely nitrogen limited) are always subject to successful invasion by strategies that will generate open-canopy conditions when they become residents. (5) Up to the point of nitrogen saturation, ESS allocation to foliage maximizes stem diameter growth rate in monoculture (i.e., is "optimal"), whereas ESS allocation to either fine roots or wood does not.

Quantitative Description of the Model

Individuals compete for soil nitrogen, with net mineralization rate N_{avail} (derived from a full nitrogen cycling model; see app. G), as a function of their fine root mass R:

$$N_{\text{X,x}} \approx \frac{R_{\text{X,x}}}{R_{\text{C,r}}} N_{\text{avail}}, \tag{1}$$

where $N_{\text{X,x}}$ is the nitrogen acquired by an individual per unit projected crown area. Following a system of subscripts that will be used again below, equation (1) can be used to calculate the per crown area nitrogen uptake of either understory or canopy individuals of either the resident or

invader strategies by substituting X with either U (understory) or C (canopy) and x with either r (resident) or m (invader). The equation states that an individual's nitrogen acquisition is proportional to the nitrogen mineralization rate and its fine root mass, relative to the resident's canopy fine root mass.

Because of stoichiometric constraints on the construction of foliage, individuals that acquire more nitrogen ($N_{X,x}$; eq. [1]) can build more leaf layers (fig. 1; cf. depth of circled invader foliage to resident foliage):

$$L_{X,x} \leq \frac{N_{X,x}\rho}{\delta_L \gamma_L f}, \tag{2}$$

where $L_{X,x}$ is the one-sided leaf area per ground area of an individual (LAI), $N_{X,x}$ is determined by $R_{X,x}$ via equation (1), ρ is the fraction of nitrogen taken up that is allocated to foliage, δ_L is the nitrogen concentration of leaves per unit area (although this value is clearly different for sun leaves and shade leaves even within the same individual, we assume for simplicity no change in δ_L), f is the fraction of nitrogen lost from senesced foliage, and γ_L is leaf turnover. Note that in contrast to empirical measures of LAI, which are made at the ecosystem level, we define LAI at the individual level. However, our definition of LAI for canopy individuals will closely accord with empirical measurements in closed-canopy forests where total projected crown area and/or LAI of understory individuals is small. The inequality in equation (2) states that an individual can build less foliage than it has nitrogen for, but we show in the results that this is never adaptive for a nitrogen-limited plant and so equation (2) is more usefully understood with a strict equality under nitrogen-limited conditions.

Because light is directional, individuals shade their own leaves and the leaves of trees below them. If I_X^0 is the light intensity at the top of an individual, $L_{X,x}$ is its uniform LAI, and k is the light extinction coefficient, then the light intensity incident on its lowest leaves diminishes exponentially as a function of the leaves above:

$$I_{X,x}^{\text{bottom}} = I_X^0 e^{-kL_{X,x}}. \tag{3}$$

The light intensity at the top of the canopy is taken as full sun, I_C^0, whereas the light intensity at the top of the understory diminishes exponentially as a function of the canopy's LAI:

$$I_U^0 = I_C^0 e^{-kL_{C,r}\zeta}. \tag{4}$$

The parameter ζ is between 0 and 1 and phenomenologically accounts for both small-scale disturbance mechanisms (e.g., single tree-fall gaps, branch breakage) and wind-driven canopy crown movements (synchronous within individuals but asynchronous among individuals) that can cause understory light intensities to exceed those of the lowest canopy leaves.

The rate of carbon gain by a tree's crown is the sum of the photosynthetic rates of its leaf layers. Net photosynthetic rates (photosynthesis minus leaf maintenance respiration) are governed by the function in figure 2. In full sun, leaves photosynthesize at the maximum rate, but that rate diminishes in lower leaves due to self-shading (fig. 1, depicted as a gradient within each crown; fig. 2). In addition to self-shading, the photosynthesis of understory individuals is reduced by the shade of the canopy individuals above them (fig. 1; eq. [4]). There are three distinct cases, depending on whether portions of $L_{X,x}$ are light saturated, partly light saturated and partly light limited, or solely light limited. The light intensity at which a leaf transitions from light saturated to light limited is $\tilde{I} = (A_{\max} + q)/\Phi$ (fig. 2), where $A_{\max}$ is the maximum photosynthetic rate, q is the dark respiration rate, and Φ is the quantum yield of light-limited photosynthesis. In the first case, the entire $L_{X,x}$ (determined by eq. [2]) is light saturated, such that $I_X^0 > \tilde{I}$ and $I_{X,x}^{\text{bottom}} \geq \tilde{I}$ and per–projected crown area net photosynthesis is

$$E_{X,x} = sA_{\max}L_{X,x}, \tag{5}$$

where s scales per-second rates to yearly rates. In the second case, part of the $L_{X,x}$ is light saturated and part is light limited, such that $I_X^0 > \tilde{I}$ and $I_{X,x}^{\text{bottom}} < \tilde{I}$:

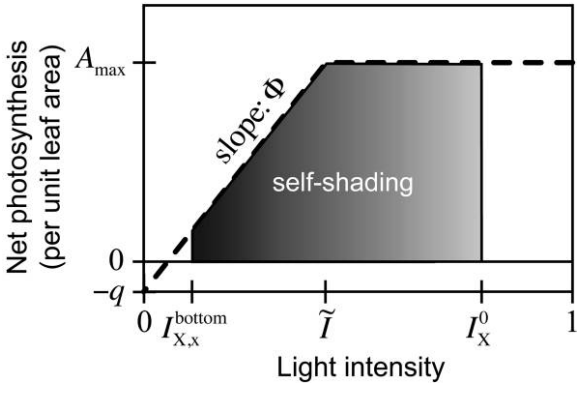

Figure 2: Simplified model of net photosynthesis, with the X-axis running from completely dark (*left*) to completely bright (*right*). Net photosynthesis is calculated by integrating across $L_{X,x}$ from I_X^0 to $I_{X,x}^{\text{bottom}}$, where $I_{X,x}^{\text{bottom}}$ is determined by self-shading. I_X^0 and $I_{X,x}^{\text{bottom}}$ are free to vary along the X-axis, provided $I_X^0 > I_{X,x}^{\text{bottom}}$. $\tilde{I}$ defines the transition light level between light limited and light saturated and is equal to $(A_{\max} + q)/\phi$.

$$E_{\mathrm{X,x}} = s\left\{\frac{A_{\max} + q}{k}\left[1 + \ln\left(\frac{\Phi I_{\mathrm{X}}^{0}}{A_{\max} + q}\right)\right] - \frac{\Phi I_{\mathrm{X}}^{0}}{k} e^{-kL_{\mathrm{X,x}}} - qL_{\mathrm{X,x}}\right\}. \quad (6)$$

In the third and final case, all of the $L_{\mathrm{X,x}}$ is light limited, such that $I_{\mathrm{X}}^{0} < \tilde{I}$

$$E_{\mathrm{X,x}} = s\left[\frac{\Phi I_{\mathrm{X}}^{0}}{k}(1 - e^{-kL_{\mathrm{X,x}}}) - qL_{\mathrm{X,x}}\right]. \quad (7)$$

We note that in our treatment we always assume that $I_{\mathrm{C}}^{0} > \tilde{I}$, and thus, canopy trees are never solely light limited. In contrast, because light at the top of understory individuals is reduced by the canopy's shade, understory individuals are often partially light saturated and partially light limited or solely light limited. We use the terms "nitrogen limited" (eq. [5]), "light limited" (eq. [7]), and "dual limited" (eq. [6] or eq. [7]) to reflect their empirical interpretations, where adding only nitrogen, only light, or either nitrogen or light, respectively, would increase growth rates. To be clear, a dual-limited individual would benefit from the addition of nitrogen by itself, light by itself, or both together. All other resources, including water and phosphorus, are assumed to be nonlimiting regardless of allocation.

We assume that individuals allocate fixed carbon to support foliage, fine roots, reproductive structures (if they are in the canopy), and structural wood (branches, stem, and coarse roots). This implies diameter growth rate (see app. G):

$$G_{\mathrm{X,x}} \approx \frac{\pi\alpha^{\theta}}{(\theta + 1)a}\{E_{\mathrm{X,x}} - (1 + \kappa_{\mathrm{L}})\gamma_{\mathrm{L}}ML_{\mathrm{X,x}} - [(1 + \kappa_{\mathrm{R}})\gamma_{\mathrm{R}} + \Omega]R_{\mathrm{X,x}} - \omega_{\mathrm{C}}\}, \quad (8)$$

where α, a, and θ are all allometric constants that relate stem diameter to projected crown area and total tree mass (see app. G); $E_{\mathrm{X,x}}$ is determined by equation [5], [6], or [7], depending on the environment; γ_{L} is leaf turnover; M is leaf carbon per one-sided leaf area; κ_{L} is the respiratory cost of building leaves; γ_{R} is fine root turnover; κ_{R} is the respiratory cost of building fine roots; Ω is the maintenance respiration rate of fine roots; and ω_{C} is the annual build and maintenance cost of fecundity per projected crown area. Equation (8) states that stem diameter growth rate is proportional to net photosynthesis (first term) minus the build cost of foliage (second term) minus the build and respiratory cost of fine roots (third term) minus allocation to fecundity (last term), scaled by allometric constants. The equation does not include foliage maintenance respiration, as this is already subsumed in the calculation of net photosynthetic rate, $E_{\mathrm{X,x}}$. We assume negligible wood turnover and respiration. As developed in appendix G, allocation to wood is directly proportional to the stem diameter growth rate $G_{\mathrm{X,x}}$ (and, via allometry, to the height growth rate). As a consequence of the allometric equations that we use and justify in online appendixes A and G, stem diameter growth rates, $G_{\mathrm{X,x}}$, are constant and independent of stem diameter.

The methods of the perfect plasticity approximation, which classify individual trees as being in the canopy (as tall as or taller than the minimum canopy crown height; $\tilde{Z}_{\mathrm{r}}$; fig. 1) or in the understory (shorter than $\tilde{Z}_{\mathrm{r}}$; fig. 1) without reference to their spatial locations, allow us to rigorously scale up the individual-level ecology presented above to the community level (Adams et al. 2007; Strigul et al. 2008). Assuming the same height allometries among species, as we do here, the stem diameter $\tilde{D}_{\mathrm{r}}$ that corresponds to $\tilde{Z}_{\mathrm{r}}$ for an equilibrial monoculture is approximately

$$\tilde{D}_{\mathrm{r}} \approx \frac{G_{\mathrm{U,x}}}{\mu_{\mathrm{U}}} \ln\left[F\pi\alpha^{\theta}\Gamma(\theta + 1)\frac{G_{\mathrm{C,r}}^{\theta}}{\mu_{\mathrm{C}}^{\theta+1}}\right], \quad (9)$$

where μ_{C} and μ_{U} are canopy and understory mortality rates, F is per–ground area fecundity, $\Gamma(\ldots)$ is the gamma function, α and θ relate projected crown area to stem diameter, and $G_{\mathrm{U,r}}$ and $G_{\mathrm{C,r}}$ are determined by equation (8). As revealed in equation (9), $\tilde{D}_{\mathrm{r}}$ increases with growth rates and fecundity and decreases with mortality rates in a way that properly weights the understory and canopy components (Strigul et al. 2008).The lifetime reproductive success, or fitness W_{x}, of a strategy is approximately

$$W_{\mathrm{x}} \approx e^{-\tilde{D}_{\mathrm{r}}(\mu_{\mathrm{U}}/G_{\mathrm{U,x}})}F\pi\alpha^{\theta}\frac{G_{\mathrm{C,x}}^{\theta}}{\mu_{\mathrm{C}}^{\theta+1}}\Gamma(\theta + 1), \quad (10)$$

where $G_{\mathrm{U,x}}$ and $G_{\mathrm{C,x}}$ are determined by equation (8). We restrict our analysis to cases that result in closed-canopy forests, for which $G_{\mathrm{U,x}}$ and $G_{\mathrm{C,x}}$ are necessarily greater than 0. As described in appendix G, we use slightly more accurate but more cumbersome expressions for determining numerical results in figures. Qualitative results are not at all affected by this difference.

We use adaptive dynamics (Geritz et al. 1998; McGill and Brown 2007) to determine the most competitive allocations to foliage, wood, and fine roots for a given nitrogen availability, which we usefully characterize as individual leaf area index L_{X}^{*}, individual stem diameter growth rate (which is directly proportional to wood allocation) G_{X}^{*}, and fine root mass R_{X}^{*}. We use the term "strategy" to refer to a particular suite of such allocations. For a particular trait v we implicitly find the ESS v^{*} by finding the maxima of the fitness function W_{m} for v:

$$\left.\frac{dW_{\mathrm{m}}(\nu_{\mathrm{m}}, \nu_{\mathrm{r}})}{d\nu_{\mathrm{m}}}\right|_{\nu_{\mathrm{m}}=\nu_{\mathrm{r}},\, \nu_{\mathrm{r}}=\nu^{*}} = 0,$$

$$\left.\frac{dW_{\mathrm{m}}^{2}(\nu_{\mathrm{m}}, \nu_{\mathrm{r}})}{d^{2}\nu_{\mathrm{m}}}\right|_{\nu_{\mathrm{m}}=\nu_{\mathrm{r}},\, \nu_{\mathrm{r}}=\nu^{*}} < 0, \qquad (11)$$

where W_{m} is a function of both the invader's strategy ν_{m} and the resident's strategy ν_{r} and is both continuous and smooth within the domain of analysis (Geritz et al. 1998; McGill and Brown 2007). Because of their functional connection to $G_{\mathrm{X,x}}$ (eq. [8]), L_{X}^{*} and R_{X}^{*} uniquely determine G_{X}^{*}; although it is vastly more cumbersome, we could obtain the same numerical results by solving first for L_{X}^{*} and G_{X}^{*} and then substituting them for R_{X}^{*}. Equation (11) identifies local ESS candidate strategies that, as residents, are uninvadible by nearby strategies. We determine that these ESS candidate strategies are both global and convergent stable in appendix F in the online edition of the *American Naturalist*.

By subtracting carbon consumed by respiration, our growth equation (eq. [8]) lends itself to comparison with empirical net primary productivity (NPP) measurements:

$$\begin{aligned}
\mathrm{NPP}_{\mathrm{foliage}} &\equiv \gamma_{\mathrm{L}} M L_{\mathrm{X,x}},\\
\mathrm{NPP}_{\mathrm{wood}} &= \left[\frac{\pi\alpha^{\theta}}{(\theta+1)a}\right]^{-1} G_{\mathrm{X,x}},\\
\mathrm{NPP}_{\mathrm{aboveground\ wood}} &= \left[\frac{\pi\alpha^{\theta}}{(\theta+1)a}\right]^{-1} \Lambda G_{\mathrm{X,x}}, \qquad (12)\\
\mathrm{NPP}_{\mathrm{fine\ root}} &\equiv \gamma_{\mathrm{R}} R_{\mathrm{X,x}},
\end{aligned}$$

where Λ is the fraction of wood allocated aboveground. All four values are expressed in common units ($\mathrm{g_{carbon}\ m^{-2}\ year^{-1}}$ for our parameterization; table 1). Relative NPP of any component is found by dividing it by the sum of $\mathrm{NPP_{foliage}}$, $\mathrm{NPP_{wood}}$, and $\mathrm{NPP_{fine\ root}}$.

Analytical and Quantitative Results

Appendix G contains the derivations and additional explanations for the following results.

Result 1

Increasing ESS foliage with increasing nitrogen availability. Across a fertility gradient, as N_{avail} increases, the most competitive LAIs in both the canopy, L_{C}^{*}, and in the understory, L_{U}^{*}, increase up to the point of nitrogen saturation (fig. 3). First, we find the ESS, assuming that nitrogen is unlimited:

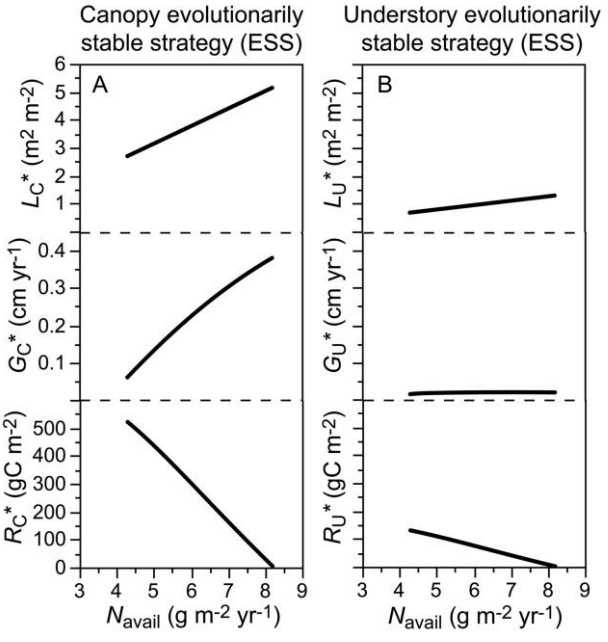

Figure 3: The evolutionarily stable strategy leaf area index (L_{X}^{*}), stem growth rate (G_{X}^{*}), and fine root mass (R_{X}^{*}) across a nitrogen availability gradient for canopy (*A*) and understory (*B*) individuals. Lines begin at low N_{avail} as growth rates become sufficient to allow for closed-canopy forest. Lines end at high N_{avail} as foliage becomes nitrogen saturated, where additional nitrogen uptake would be neither competitive nor optimal and where we thus expect nitrogen to leach from the system.

$$L_{\mathrm{C}}^{*\mathrm{sat}} = \frac{1}{k}\ln\left[\frac{s\Phi I_{\mathrm{C}}^{0}}{(1+\kappa_{\mathrm{L}})\gamma_{\mathrm{L}} M + sq}\right], \qquad (13)$$

where "sat" indicates that this is the nitrogen-saturated result. Interpretation of this equation is straightforward. The most competitive nitrogen-saturated LAI, $L_{\mathrm{C}}^{*\mathrm{sat}}$, depends strongly on k, the light extinction coefficient; smaller k leads to greater $L_{\mathrm{C}}^{*\mathrm{sat}}$ because it decreases self-shading. Of those variables that may vary appreciably among species or habitats, increased $L_{\mathrm{C}}^{*\mathrm{sat}}$ occurs with increasing extrapolated net photosynthetic rate s or decreasing leaf turnover rate γ_{L}, leaf carbon per area M, or leaf dark respiration rate q. Because A_{max} and q are often positively correlated, decreasing A_{max} will likely increase $L_{\mathrm{C}}^{*\mathrm{sat}}$. At $L_{\mathrm{C}}^{*\mathrm{sat}}$, the lowest leaves of canopy trees are just able to pay for their own construction and respiratory costs. This is an upper limit, as it does not take into account the possibility that additional whole-plant respiratory costs are required to support those lowest leaves (Reich et al. 2009). It is easy to show that in habitats with less-than-saturating nitrogen

availability, a strategy that builds as much foliage as it can (according to eq. [2]) will invade a strategy that builds $L_{C,r}$ less than that (see derivation of result 5 in app. G). Thus,

$$L_C^* = \min\left(\frac{N_{avail}\rho}{\delta_L \gamma_L f}, L_C^{*sat}\right), \quad (14)$$

where L_C^{*sat} is defined by equation (13). Parallel results hold for the understory and are detailed in appendix G. Together, these results show that the most competitive L_X^* strategy is that which builds as much foliage as it has nitrogen for, up to the point at which additional leaves would fail to pay for themselves due to self-shading.

Result 2

Decreasing ESS fine root mass with increasing nitrogen availability. Across a soil fertility gradient as N_{avail} increases, the most competitive fine root mass, R_X^*, decreases monotonically. No closed-canopy R_X^* exists at low N_{avail} because successful invaders with greater $R_{C,m}$ drive the system into open-canopy, nonforest conditions (see app. C in the online edition of the *American Naturalist*). For all N_{avail} sufficiently large, a stable R_X^* exists up to the point at which the canopy becomes nitrogen saturated (fig. 3). Here we show the canopy ESS R_C^*; the understory ESS is similar and is detailed in appendix G:

$$R_C^* = \frac{s\Phi I_C^0 e^{-kL_C^*} - sq - (1+\kappa_L)\gamma_L M}{(1+\kappa_R)\gamma_R + \Omega} L_C^*. \quad (15)$$

Equation (15) is a ratio. The quantum yield, Φ, is the slope of light-limited photosynthesis with light availability (fig. 2) and $I_C^0 \exp(-kL_C^*)$ is light availability at the lowest leaf layer. Thus, the first term in the numerator describes the rate of light-limited photosynthesis at the lowest leaf layer. The second and third terms in the numerator are the respiratory and build costs of that leaf layer. Together, the numerator is the net marginal carbon benefit given to an invader with greater fine root mass than the resident. Whenever an individual is at least partially light limited, this marginal benefit will decrease with N_{avail} because L_C^* increases and thus the light at the bottom of the canopy due to self-shading will decrease. The denominator for R_C^* is the fixed carbon cost of that infinitesimally greater root investment. In contrast to the numerator, this fixed root cost never varies with N_{avail}. Simply put, R_C^* decreases with N_{avail} because the marginal benefit to greater root investment decreases due to self-shading while the cost remains fixed. It is easy to show that R_C^* goes to 0 as L_C^* goes to L_C^{*sat} (eq. [13]), demonstrating that the premium paid on fine root biomass for the purpose of nitrogen uptake goes to 0 as nitrogen becomes nonlimiting (assuming, as we do, no leaching of nitrogen).

Result 3

Increasing ESS growth rates with increasing nitrogen availability. The most competitive growth rate in the canopy, G_C^*, increases monotonically and saturates with increasing N_{avail}:

$$G_C^* = \frac{\pi\alpha^\theta}{(\theta+1)a}\left\{\frac{(A_{max}+q)s}{k}\left[1+\ln\left(\frac{\Phi I_C^0}{A_{max}+q}\right)\right] - (kL_C^*+1)\frac{s\Phi I_C^0}{k}e^{-kL_C^*} - \omega_C\right\}. \quad (16)$$

Over the range of N_{avail} for which the model predicts closed-canopy forest, the term involving the exponent becomes less negative with increasing N_{avail}, causing the whole function to increase but in a saturating way. Apart from the conversion constants in front and the cost of fecundity, equation (16) differs from the equation for net photosynthesis (eq. [6]) by the addition of kL_C^* to the term involving the exponent, which effectively incorporates the increasing cost of L_C^* and the decreasing cost of R_C^* with N_{avail}. It is also possible to solve analytically for G_U^*, but the resulting expression is neither simple nor illuminating.

Result 4

Forests composed of individuals with ESSs are dual limited up to the point of nitrogen saturation. Up to the point of nitrogen saturation, where no tree in a stand is limited by nitrogen, our model predicts that all ESS forests are dual limited; that is, the canopy, and sometimes the understory, is limited by both nitrogen and light. At low N_{avail}, where both the canopy and understory would be solely nitrogen limited, no ESS closed-canopy forest can exist, because strategies that lead to open-canopy conditions always successfully invade closed-canopy strategies (app. C). Only after the canopy becomes dual limited with increasing N_{avail} does the possibility exist for an ESS closed-canopy forest. As N_{avail} increases, the understory transitions from dual limited to solely light limited. At the point of nitrogen saturation, no individual is limited by nitrogen, and both the understory and canopy are at L_X^{*sat} (eq. [13]; app. G).

Result 5

Under nitrogen-limited conditions, ESS foliage maximizes competitive ability and stem growth rate in monoculture (i.e., is "optimal"), whereas ESS fine root mass and wood allocation maximize only competitive ability (i.e., are not "op-

timal"). By design, our method for determining ESSs (eq. [11]) finds those strategies that are uninvadible and thus the most competitive among all neighboring strategies. In much of the literature on plant ecology, plants are assumed to maximize carbon gain or individual growth rate in monoculture or in the absence of competition; that is, they are said to be "optimal." In addition to being the most competitive strategy, ESS foliage L_C^* is optimal in this sense, but ESS fine root mass and growth rate, R_C^* and G_C^*, are not.

Model Predictions Compared to Empirical NPP Data

We compared our model predictions of NPP, both relative and absolute, to data from the FLUXNET database (Luyssaert et al. 2007) and Santantonio (1989); details can be found in appendix D in the online edition of the *American Naturalist*. We used common units (g C m^{-2} $year^{-1}$) for foliage, aboveground wood, and fine roots NPP as described in equation [12]. No part of the model, either its formulation or its parameterization, was based on these data, and the lines are generated as ESS solutions to the model, not as statistical fits to the data (i.e., the lines are generated without any reference to the data at all).

Both the data and our model's predictions reveal a strong negative relationship between fractional NPP of wood and fine roots but very little relationship between fractional NPP of either wood and foliage or fine roots and foliage (fig. 4). The model's predictions are close to the empirical relationship (i.e., regression line, not shown) and most of the range of the fractional data (fig. 4). Not surprisingly, the data reveal increasing absolute NPP of foliage, wood, and fine roots with increasing total NPP (fig. 5). The model's predictions largely fall within the range of the absolute data but fail to find the empirical relationships (i.e., regression lines, not shown) or generate values for large ranges of the observed data (fig. 5). Moreover, whereas the data show a generally positive relationship between absolute NPP of fine roots and total NPP, the model predicts a negative relationship (fig. 5).

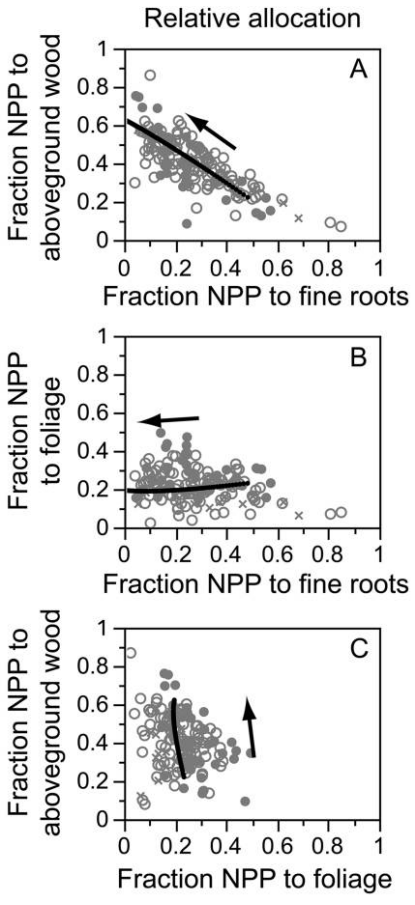

Figure 4: Empirical relations between relative net primary productivity (NPP) allocated to foliage, fine roots, and aboveground wood (*gray*) compared to independent model predictions of evolutionarily stable strategies across a nitrogen gradient. Arrows show gradient of increasing N_{avail} for model predictions. Circles represent data from the publicly available FLUXNET database (Luyssaert et al. 2007), and Xs represent data from Santantonio (1989). Stands represented by open circles or Xs are dominated by gymnosperms, whereas those represented by filled circles are dominated by angiosperms. Methodological details can be found in appendix D in the online editio nof the *American Naturalist*. These empirical data neither informed model parameters nor constrained the predictions and thus represent an independent test of the model.

Discussion

Allocational Strategies Are Not Necessarily "Optimal"

Many investigators have suggested and observed that proportional allocations to foliage and stem increase and allocation to fine roots decreases with increasing nitrogen availability in both forests and other types of vegetation (Miller and Miller 1976; Aber et al. 1985; Vogt et al. 1987; Tilman 1988; Santantonio 1989; Gholz et al. 1991; Gower et al. 1992; Reynolds and Pacala 1993; Rees and Bergelson 1997; Coomes and Grubb 2000; Jimenez et al. 2009). The suggested and observed distributions of standing biomass often follow the same patterns. These trends have been explained using optimization theory: optimal plants are said to allocate so that they balance their belowground and aboveground limitations and thus maximize growth rates (Poorter and Nagel 2000). In such a framework, the tradeoff is between belowground and aboveground resource acquisition, where capturing more of one resource necessarily means capturing less of the other (e.g., Tilman 1988; Reynolds and Pacala 1993; Aikio and Markkola 2002; Smith and Sibly 2008).

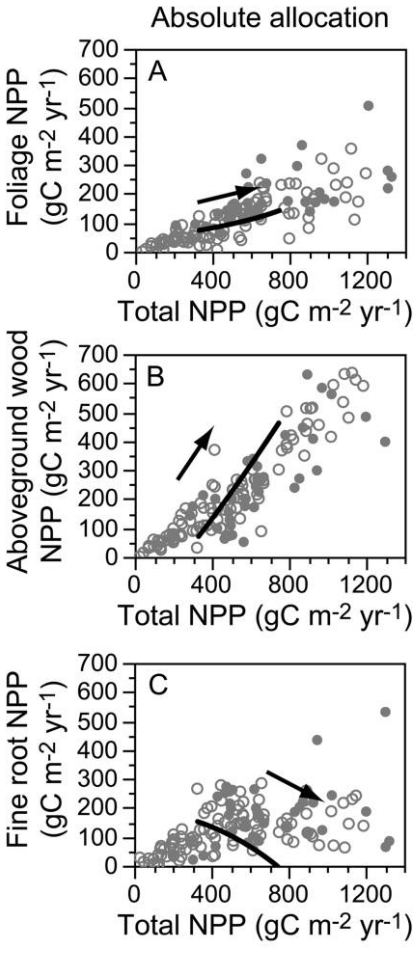

Figure 5: Empirical relations between absolute net primary productivity (NPP) allocated to foliage, aboveground wood, and fine roots (*gray*) compared to independent model predictions of evolutionarily stable strategies across a nitrogen gradient. Arrows show gradient of increasing N_{avail} for model predictions. Five data are omitted from *B* ([1,710, 900], [1,720, 1,078], [1,314, 989], [1,333, 931], [1,711, 1,299]) to increase resolution. See figure 4 legend for additional details. These empirical data neither informed model parameters nor constrained the predictions and thus represent an independent test of the model.

We believe this explanation falls short for two reasons. First, the most competitive strategies may not optimize growth rates in monoculture ("Result 5"). For example, in our model the ESS fine root and wood allocation strategies are the most competitive, in the sense that no other strategy can invade a monoculture that uses them. But they do not optimize growth rates in monoculture; strategies that allocate less to fine roots will lead to greater growth rates ("Result 5"). This objection is not specific to our model, closed-canopy forests, or even the plant kingdom (Falster and Westoby 2003): what matters is not that an ESS monoculture resident maximizes its own growth rate but that it creates conditions in which no other strategy can maintain a greater growth rate (or more accurately, greater fitness) than the ESS resident.

Second, the explanation focuses on fractional allocation, which can be a useful way to understand both within-individual carbon budgeting and responses to multiple resource limitations. Nevertheless, it is absolute allocation that determines resource acquisition for both trees and other types of vegetation. It is the absolute size (or density or area) of a root system that determines its ability to capture nitrogen, not its size relative to the rest of the plant. Similarly, it is the absolute size and height of the light intercepting organs that determine carbon capture, not their size or height relative to the rest of the plant. Moreover, there is no necessary trade-off between absolute allocation to roots and shoots in competition; greater absolute investment in roots may indirectly lead to greater absolute investment in shoots (e.g., by acquiring greater amounts of limiting nutrients that allow greater overall productivity) and vice versa.

The Ecology of ESS Allocational Strategies

It is easy to understand why the amount of foliage increases with nitrogen availability under nitrogen-limited conditions: because foliage is stoichiometrically constrained by nitrogen availability, greater nitrogen availability allows for more foliage, which leads to greater carbon fixation. Greater carbon fixation leads to greater growth rates. This is true not just of the trees that we have modeled but of any nitrogen-limited vegetation. Self-shading diminishes the relative worth of lower leaves without an equal reduction in their carbon build cost, and a plant should not build or maintain lower leaves with negative carbon balance (Givnish 1988; Anten and Poorter 2009; Reich et al. 2009). In our model, this point is described by L_X^{*sat} (eq. [13]; app. G), the most competitive LAI of a nitrogen-saturated tree. Although we have neglected it in our model, trees also modify within-canopy physiology and morphology, building a continuum between "sun leaves" and "shade leaves," which serves to increase L_X^{*sat}. But there exist light levels below which even the best-adapted and acclimated shade leaf will fail to be productive, indicating that L_X^{*sat} must exist, even allowing for within-canopy changes in physiology and morphology. Because increasing productivity due to, for instance, longer growing season length or less water limitation allows a given leaf to increase its photosynthetic gain without appreciably affecting its build cost, our model predicts greater L_X^{*sat} for trees with greater maximum annual net photosynthetic rate (s).

The reason for the decrease in fine root mass with increasing nitrogen availability (fig. 3; eq. [15]; app. G) is

important, nonobvious, and, we believe, likely to underpin competitive interactions in any plant community in which individuals are dual limited by nitrogen and light. Simply put, better nitrogen competitors (strategies of greater fine root mass) are able to build more leaves than a resident that is a poorer nitrogen competitor, but they receive less payoff for their greater fine root investment when the only "extra" leaves they can build relative to the resident are light limited. That payoff becomes smaller as the "extra" leaves become progressively more light limited, and as a consequence, ESS fine root allocation declines with increasing nitrogen availability.

As we discuss below, our model's prediction of decreasing fine root mass with increasing nitrogen availability is contradicted by the FLUXNET data (fig. 5*C*), and many empirical papers that have been published on this topic (Brassard et al. 2009). But the prediction is also supported by an approximately equal number of empirical papers, reflecting a well-known paradox of generality that awaits resolution (Brassard et al. 2009). We hope that our model may provide a path forward in this debate and that relaxing the universe of parameters that we currently hold constant (e.g., fine root turnover, annual net photosynthetic rate) with appropriate trade-offs will reveal the conditions under which to expect one or the other response. Our model makes the obviously wrong prediction that fine root mass should actually go to 0 (and not just some small but positive value) at the point of nitrogen saturation. This is a consequence of our assumptions that all other resources (including water) are abundant, independent of allocation, and that nitrogen does not leach from the system. This obvious disagreement with observation argues for a full water-nitrogen-light model.

There are interesting biological reasons for the result that ESS allocation to foliage maximizes growth rates in monoculture (i.e., is "optimal"), whereas ESS allocations to fine roots and wood do not ("Result 5"). It is easy to observe that individual tree crowns in closed-canopy forests overlap very little (Putz et al. 1984; Purves et al. 2007), such that each individual holds an independent light-intercepting "territory" for the strong vertical component of sunlight, presumably because interdigitating branches with neighbors leads to damage in wind storms. It is much less easy to observe but nonetheless true that individual tree roots overlap substantially (Gilman 1988; Stone and Kalisz 1991; Casper et al. 2003; Gottlicher et al. 2008) presumably because, in the conspicuous absence of underground wind storms, it is better to situate a new fine root in the nitrogen diffusion zone of a neighbor's fine root to "steal" nitrogen that would have otherwise gone to the neighbor (O'Brien et al. 2007). This "mean field" nature of root competition effectively forces competitive plants to divert carbon that could have gone to growth (or fecundity) in order to maintain an environment that prevents would-be usurpers from deriving any net benefit by playing a different strategy.

In contrast to models that assume that the most competitive strategies are those that maximize growth rates in monoculture, our analysis reveals that low-nitrogen systems, in which all of the closed-canopy foliage is light saturated, will always be invasible by strategies that invest so heavily in fine roots that when they become residents, their growth rates, relative to mortality rates, are too slow to close the canopy (app. C). Thus, at low nitrogen availability, our model predicts that extant closed-canopy forests must necessarily be dual limited by nitrogen and light. At high nitrogen availability, a closed-canopy forest eventually becomes nitrogen saturated, where there exists no reason, either competitive or optimal, for trees to take up the additional nitrogen. If trees can avoid luxury consumption of nitrogen (which incurs costs for conversion from mineral form and storage), we expect nitrogen-saturated forests to leach nitrogen until what remains just meets the nitrogen-saturated demand. Such a forest would be solely light limited but balanced at the brink of dual limitation with nitrogen as well. An extensive study of 50 stands of various compositions in the middle United States revealed no evidence of nitrogen saturation (Reich et al. 1997). In a forest nitrogen addition experiment, Perakis et al. (2005) found a threshold nitrogen addition rate that stimulated leaching, consistent with our conjecture.

Empirical Patterns in Allocation

With changes in nitrogen availability alone, our model predicts the major quantitative trends in fractional allocation to foliage, wood, and fine roots in the data of FLUXNET (Luyssaert et al. 2007) and Santantonio (1989). The fractional allocations in both the data and our predictions reveal a strong structural trade-off between carbon allocated to fine roots and wood (fig. 4*A*) but very little structural trade-off between foliage and either fine roots (fig. 4*B*) or wood (fig. 4*C*). Our model provides an explanation for this.

The model predicts that trees should allocate carbon to foliage in proportion to the nitrogen they acquire, up to the point at which the lowest and most shaded leaves would fail to pay for themselves in carbon (eq. [14]). Because almost all mineralized nitrogen (net after microbial immobilization) is taken up quickly by nitrogen-limited trees, independent of fine root mass (Raynaud and Leadley 2004), our model predicts that allocation to fine root and foliage should be independent. Because that foliage more than pays for itself, such a "decision" is beneficial, fixing more net carbon to pay for fine roots, fecundity, or growth at the timescale of a season than would

have been available if the initial carbon had originally been invested directly in fine roots, fecundity, or growth. Note that this may not be true of other plant forms, such as annuals, that are incapable of storing enough labile carbon to deploy a full leaf complement at the onset of the growing season. In contrast to foliage, our model predicts that carbon allocation to fine roots and wood, both of which are solely carbon sinks, should negatively covary. Because fecundity is almost entirely a carbon sink, albeit often small, the full trade-off is likely between fine roots, wood, and fecundity.

Santantonio's (1989) analysis of his smaller subset of the data included site conditions, and he found that stands with greater fractional fine root allocation were associated with sites that were less favorable for growth, consistent with our model predictions (notice N_{avail} arrow in fig. 4*A*). Similarly, among 14 oak woodlands, Reich (2002) observed greater fractional fine root allocation associated with sites with lower soil N availability. In contrast to optimization models, which predict that plants should increase allocation to capture the more limiting resource (e.g., Reynolds and Pacala 1993; Poorter and Nagel 2000; Aikio and Markkola 2002), our model predicts that increased shade should decrease allocation to foliage, if anything (consider I_X^0 in eq. [14]; app. G). Consistent with our model prediction, Reich (2002) summarized a number of studies in which experimental shading resulted not in greater leaf mass fraction but rather increased allocation to stem at the expense of roots. We suggest that a casual interpretation of the "root-shoot" trade-off as involving foliage should be more rigorously characterized as a "root-stem" trade-off, or more rigorously still as a "fine root–wood" trade-off, at least for long-lived trees.

The model's ability to predict patterns in absolute allocation of foliage and wood (fig. 5) is, on the one hand, remarkable for a model that is simple enough to yield analytical solutions and that by design ignores some well-known and often highly influential processes (e.g., variations in physiology, water availability, and season length). With earlier analytical models (e.g., Reynolds and Pacala 1993), one could not have even attempted a quantitative prediction of this nature, let alone come close to succeeding. On the other hand, as parameterized, the model does not predict closed-canopy forests of either low or high total NPP (fig. 5); it makes predictions that appear far from the empirical relationships (i.e., fit regression lines, not shown) for both foliage NPP (fig. 5*A*) and aboveground wood NPP (fig. 5*B*); and it predicts decreasing fine root NPP with increasing total NPP, in opposition to the dominant increasing trend (fig. 5*C*). Clearly, shifts in allocation along nitrogen gradients explain some of the variation in the data, but their failure to account for much of it is consistent with the notion that competitive shifts in physiology and within-organ morphology, as well as limitation by other resources (none of which we have considered here) are of great importance.

The data contain stands with lower productivity than even our lowest predicted closed-canopy stand (~300 g C m^{-2} $year^{-1}$), but all of those stands are dominated by conifers. Our model is parameterized for temperate deciduous broadleaf species (table 1), and thus our inability to predict those low-productivity conifer sites highlights the important differences between the two taxa. Several of our predictions fall outside the range of observed allocations because our model makes the wrong prediction that fine root mass should fall to 0 at high nitrogen availability. In reality, fine root mass should be low, but not 0, at high nitrogen availability because even abundant nitrogen requires a mechanism of uptake and, in addition, fine roots are responsible for the uptake of other resources. Raising the high nitrogen availability predictions of fine root mass would bring the predictions into better agreement with the data, which highlights the importance of incorporating potential limitation by other resources into the model.

It is curious that the model predicts decreasing fine root NPP with increasing total NPP, whereas the data show a positive correlation between fine root NPP and total NPP, at least for total NPP < 700 g C m^{-2} $year^{-1}$. As mentioned above, there are echoes of such radically divergent patterns in the literature. Brassard et al. (2009) summarized numerous studies across soil nitrogen gradients that reported either significantly increasing or significantly decreasing fine root production, turnover, and biomass. By inspection of the equation for the ESS fine root allocation (eq. [15]), it is clear that several parameters would increase or decrease its value, holding nitrogen availability constant. However, *s*, the parameter that scales measured net photosynthesis per second to a yearly rate, stands out as one that is likely to shift along important gradients. We expect *s* to be positively correlated with growing season length and negatively correlated with nonnitrogen resource limitation (e.g., water). Among taxa, the parameters that describe fine root and foliage turnover, respiration, and construction costs will vary and thus affect ESS fine root allocation. Our results suggest that studies that effectively hold these parameters, including *s*, constant by controlling growing season length, taxa, and other resource limitations should observe decreasing fine root production and biomass, whereas those that allow them to vary might observe any relationship. Since soil texture, water availability, and nitrogen mineralization rates are frequently correlated (Reich et al. 1997), it may be easy to find many naturally occurring nitrogen availability gradients that are also potentially correlated gradients in these other parameters.

We simplified our model by assuming old-growth con-

ditions, but it is likely that many extant forests are still recovering from anthropogenic and natural stand-level disturbances. Indeed, the FLUXNET data set contains 62 and 24 stands that were characterized as "managed" and "recently disturbed," respectively. Nevertheless, the general allocational patterns between these and the other stands are not substantively different (app. D), suggesting that the strategies of canopy trees, which the data overwhelmingly represent, differ little across disturbance gradients. However, we do expect other aspects, including leaf physiology, wood morphology, and the importance of the understory stage, to vary between early successional and old-growth stands.

Unanswered Questions

Much remains to be understood, of course. For example, real forests are often quite diverse. Our model, like others that involve light competition (e.g., Tilman 1988; Reynolds and Pacala 1993; Rees and Bergelson 1997), does not explain this diversity without invoking exogenous mechanisms (e.g., Tilman and Pacala 1993; Fargione and Tilman 2002; Wright 2002) because it admits no local coexistence (app. F). We note that without changing our model structure, the physiological parameters that we currently treat as constants (e.g., A_{max}, M, δ_L, etc.) may also be analyzed as ESSs to reveal the competitive mechanisms that underlie physiological shifts and, potentially, local coexistence across gradients under nitrogen and light limitation.

Beyond this, the approach that we have outlined may be viewed as a special case of a more general model that will also accommodate and predict ESS traits for open-canopy conditions and plant growth forms that differ from those of trees. Unlike other approaches, ours permits smooth transitions from, for example, desert to grassland to forest, and holds the promise of a mechanistic understanding of the forces that determine the large-scale, repeatable patterns in global vegetation (and hence their mechanistically based response to global change). More broadly, we believe our formal scaling of individual-level processes and interactions to their community-, ecosystem-, and evolutionary-level consequences, may, with modifications, shed light on open questions in ecology for which the small-scale physiology and large-scale patterns are understood but for which the link between the two scales has so far lacked rigor (Givnish 2002).

Acknowledgments

We thank W. S. Harpole, S. Levin, J. Lichstein, D. Menge, and two anonymous reviewers for insightful comments that improved the paper. We are grateful to the FLUXNET network (http://www.daac.ornl.gov/FLUXNET/fluxnet.html) for making its NPP data available.

Literature Cited

Aber, J. D., J. M. Melillo, K. J. Nadelhoffer, C. A. McClaugherty, and J. Pastor. 1985. Fine root turnover in forest ecosystems in relation to quantity and form of nitrogen availability: a comparison of two methods. Oecologia (Berlin) 66:317–321.

Adams, T. P., D. W. Purves, and S. W. Pacala. 2007. Understanding height-structured competition in forests: is there an R^* for light? Proceedings of the Royal Society B: Biological Sciences 274:3039–3047.

Aikio, S., and A. M. Markkola. 2002. Optimality and phenotypic plasticity of shoot-to-root ratio under variable light and nutrient availabilities. Evolutionary Ecology 16:67–76.

Anten, N. P. R., and H. Poorter. 2009. Carbon balance of the oldest and most-shaded leaves in a vegetation: a litmus test for canopy models. New Phytologist 183:1–3.

Brassard, B. W., H. Y. H. Chen, and Y. Bergeron. 2009. Influence of environmental variability on root dynamics in northern forests. Critical Reviews in Plant Sciences 28:179–197.

Casper, B. B., H. J. Schenk, and R. B. Jackson. 2003. Defining a plant's belowground zone of influence. Ecology 84:2313–2321.

Coomes, D. A., and P. J. Grubb. 2000. Impacts of root competition in forests and woodlands: a theoretical framework and review of experiments. Ecological Monographs 70:171–207.

DeAngelis, D. L., K. A. Rose, L. B. Crowder, E. A. Marschall, and D. Lika. 1993. Fish cohort dynamics: application of complementary modeling approaches. American Naturalist 142:604–622.

De Roos, A. M., and L. Persson. 2001. Physiologically structured models: from versatile technique to ecological theory. Oikos 94: 51–71.

Di Lucca, C. M. 1998. TASS/SYLVER/TIPSY: systems for predicting the impact of silvicultural practices on yield, lumber value, economic return and other benefits. Pages 7–16 *in* C. R. Bamsey, ed. Stand density management conference: using the planning tools. Alberta Environmental Protection, Edmonton.

Falster, D. S., and M. Westoby. 2003. Plant height and evolutionary games. Trends in Ecology & Evolution 18:337–343.

Fargione, J., and D. Tilman. 2002. Competition and coexistence in terrestrial plants. Pages 165–206 *in* U. Sommer and B. Worm, eds. Competition and coexistence. Springer, Berlin.

Friedlingstein, P., G. Joel, C. B. Field, and I. Y. Fung. 1999. Toward an allocation scheme for global terrestrial carbon models. Global Change Biology 5:755–770.

Geritz, S. A. H., E. Kisdi, G. Meszena, and J. A. J. Metz. 1998. Evolutionarily singular strategies and the adaptive growth and branching of the evolutionary tree. Evolutionary Ecology 12:35–57.

Gholz, H. L., S. A. Vogel, W. P. Cropper, K. Mckelvey, K. C. Ewel, R. O. Teskey, and P. J. Curran. 1991. Dynamics of canopy structure and light interception in *Pinus elliottii* stands, north Florida. Ecological Monographs 61:33–51.

Gilman, E. F. 1988. Tree root spread in relation to branch dripline and harvestable root ball. Hortscience 23:351–353.

Givnish, T. J. 1988. Adaptation to sun and shade: a whole-plant perspective. Australian Journal of Plant Physiology 15:63–92.

———. 2002. Adaptive significance of evergreen vs. deciduous leaves: solving the triple paradox. Silva Fennica 36:703–743.

Gottlicher, S. G., A. F. S. Taylor, H. Grip, N. R. Betson, E. Valinger, M. N. Hogberg, and P. Hogberg. 2008. The lateral spread of tree root systems in boreal forests: estimates based on ^{15}N uptake and distribution of sporocarps of ectomycorrhizal fungi. Forest Ecology and Management 255:75–81.

Gower, S. T., K. A. Vogt, and C. C. Grier. 1992. Carbon dynamics of Rocky Mountain Douglas-fir: influence of water and nutrient availability. Ecological Monographs 62:43–65.

Jimenez, E. M., F. H. Moreno, M. C. Penuela, S. Patino, and J. Lloyd. 2009. Fine root dynamics for forests on contrasting soils in the Colombian Amazon. Biogeosciences 6:2809–2827.

Luyssaert, S., I. Inglima, M. Jung, A. D. Richardson, M. Reichsteins, D. Papale, S. L. Piao, et al. 2007. CO_2 balance of boreal, temperate, and tropical forests derived from a global database. Global Change Biology 13:2509–2537.

McGill, B. J., and J. S. Brown. 2007. Evolutionary game theory and adaptive dynamics of continuous traits. Annual Review of Ecology, Evolution, and Systematics 38:403–435.

Metz, J. A. J., and O. Diekmann. 1986. The dynamics of physiologically structured populations. Lecture Notes in Biomathematics. Vol. 68. Springer, Berlin.

Miller, H. G., and J. D. Miller. 1976. Effect of nitrogen supply on net primary production in Corsican pine. Journal of Applied Ecology 13:249–256.

Mitchell, K. J. 1975. Dynamics and simulated yield of Douglas-fir. Forest Science Monographs 17:1–39.

O'Brien, E. E., J. S. Brown, and J. D. Moll. 2007. Roots in space: a spatially explicit model for below-ground competition in plants. Proceedings of the Royal Society B: Biological Sciences 274:929–934.

Pacala, S. W., C. D. Canham, J. Saponara, J. A. Silander, R. K. Kobe, and E. Ribbens. 1996. Forest models defined by field measurements: estimation, error analysis and dynamics. Ecological Monographs 66:1–43.

Perakis, S. S., J. E. Compton, and L. O. Hedin. 2005. Nitrogen retention across a gradient of ^{15}N additions to an unpolluted temperate forest soil in Chile. Ecology 86:96–105.

Poorter, H., and O. Nagel. 2000. The role of biomass allocation in the growth response of plants to different levels of light, CO_2, nutrients and water: a quantitative review. Australian Journal of Plant Physiology 27:595–607.

Purves, D., and S. Pacala. 2008. Predictive models of forest dynamics. Science 320:1452–1453.

Purves, D. W., J. W. Lichstein, and S. W. Pacala. 2007. Crown plasticity and competition for canopy space: a new apatially implicit model parameterized for 250 North American tree species. PLoS ONE 2(9):e870.

Purves, D. W., J. W. Lichstein, N. Strigul, and S. W. Pacala. 2008. Predicting and understanding forest dynamics using a simple tractable model. Proceedings of the National Academy of Sciences of the USA 105:17018–17022.

Putz, F. E., G. G. Parker, and R. M. Archibald. 1984. Mechanical abrasion and intercrown spacing. American Midland Naturalist 112:24–28.

Raynaud, X., and P. W. Leadley. 2004. Soil characteristics play a key role in modeling nutrient competition in plant communities. Ecology 85:2200–2214.

Rees, M., and J. Bergelson. 1997. Asymmetric light competition and founder control in plant communities. Journal of Theoretical Biology 184:353–358.

Reich, P. B. 2002. Root-shoot relations: optimality in acclimation and adaptation or the "emperor's new clothes"? Pages 205–220 *in* Y. Waisel, A. Eshel, and U. Kafkafi, eds. Plant roots: the hidden half. Dekker, New York.

Reich, P. B., D. F. Grigal, J. D. Aber, and S. T. Gower. 1997. Nitrogen mineralization and productivity in 50 hardwood and conifer stands on diverse soils. Ecology 78:335–347.

Reich, P. B., D. S. Falster, D. S. Ellsworth, I. J. Wright, M. Westoby, J. Oleksyn, and T. D. Lee. 2009. Controls on declining carbon balance with leaf age among 10 woody species in Australian woodland: do leaves have zero daily net carbon balances when they die? New Phytologist 183:153–166.

Reynolds, H. L., and S. W. Pacala. 1993. An analytical treatment of root-shoot ratio and plant competition for soil nutrient and light. American Naturalist 141:51–70.

Santantonio, D. 1989. Dry-matter partitioning and fine-root production in forests: new approaches to a difficult problem. Pages 57–72 *in* J. S. Periera and J. J. Landsberg, eds. Biomass production by fast-growing trees. Kluwer Academic, Dordrecht.

Smith, M. J., and R. M. Sibly. 2008. Identification of trade-offs underlying the primary strategies of plants. Evolutionary Ecology Research 10:45–60.

Stone, E. L., and P. J. Kalisz. 1991. On the maximum extent of tree roots. Forest Ecology and Management 46:59–102.

Strigul, N., D. Pristinski, D. Purves, J. Dushoff, and S. Pacala. 2008. Scaling from trees to forests: tractable macroscopic equations for forest dynamics. Ecological Monographs 78:523–545.

Tilman, D. 1988. Plant strategies and the dynamics and structure of plant communities. Monographs in Population Biology. Vol. 26. Princeton University Press, Princeton, NJ.

Tilman, D., and S. Pacala. 1993. The maintenance of species richness in plant communities. Pages 13–25 *in* R. E. Ricklefs and D. Schluter, eds. Species diversity in ecological communities. University of Chicago Press, Chicago.

Umeki, K. 1995. Modeling the relationship between the asymmetry in crown display and local environment. Ecological Modelling 82: 11–20.

Vogt, K. A., D. J. Vogt, E. E. Moore, B. A. Fatuga, M. R. Redlin, and R. L. Edmonds. 1987. Conifer and angiosperm fine-root biomass in relation to stand age and site productivity in Douglas-fir forests. Journal of Ecology 75:857–870.

von Foerster, H. 1959. Some remarks on changing populations. Pages 382–407 *in* J. F. Stohlman, ed. The kinetics of cellular proliferation. Grune & Stratton, New York.

Wright, S. J. 2002. Plant diversity in tropical forests: a review of mechanisms of species coexistence. Oecologia (Berlin) 130:1–14.

Associate Editor: Christopher A. Klausmeier
Editor: Mark A. McPeek

 DOI: 10.1086/657992

Appendix A from R. Dybzinski et al., "Evolutionarily Stable Strategy Carbon Allocation to Foliage, Wood, and Fine Roots in Trees Competing for Light and Nitrogen: An Analytically Tractable, Individual-Based Model and Quantitative Comparisons to Data"

(Am. Nat., vol. 177, no. 2, p. 153)

Equating the Allometric Exponents for Power Laws: Crown Area, Mass, and Fine Root Investment

Crown Area and Mass

In this section, we demonstrate that the exponent θ, which relates individual crown area to stem diameter D, is approximately 1 less than the exponent b, which relates individual mass to stem diameter (see app. G). The carbon budget closes and modeled stem diameter growth becomes diameter independent (as observed empirically) if $b = \theta + 1$. Here, we show that this relationship appears to hold empirically. We note that several earlier versions of the perfect plasticity approximation (PPA) assume that $\theta = 2$ (Adams et al. 2007; Purves et al. 2008; Strigul et al. 2008) and thus do not include it as an explicit parameter. Its true value appears to be lower than this, however.

Here, we estimate both b and θ using published data from forests around the world (Cannell 1982). For stands that are closed canopy and composed of canopy trees of equal D, we can calculate the average projected crown area, $A(D)$ if we know the stand density n:

$$nA(D) = T^{-1}\sum_{j=1}^{n} A_j(D) \approx 1 \Rightarrow A(D) \approx \frac{1}{n}, \tag{A1}$$

where T is total habitat area. Using the equation for crown area allometry from appendix G, we can fit a linear model with slope θ to data:

$$\ln\left(\frac{1}{n}\right) \approx \ln(\pi \cdot \alpha^{\theta}) + \theta \ln(D). \tag{A2}$$

If the above assumptions are met, this is an excellent way to estimate θ because it assumes no specific geometry (as elliptical estimates do) and averages over a large number of individuals.

Similarly, we can fit a linear model with slope b to data:

$$\ln\left(\frac{B_T}{n}\right) \approx \ln(a) + b \ln(D), \tag{A3}$$

where B_T is the total stand mass.

The Cannell data collection contains information on over 1,000 stands, but not all of them have measurements of diameter at breast height (DBH) or density. Of those that do report DBH, only an average value is given. Certainly, no stand will be composed solely of individuals with exactly the same DBH, but this ideal will be closer to reality in even-aged stands. Simulations of the PPA (which can prescribe known values of θ and b) reveal that as even-aged stands mature and the standard deviation of diameter increases even beyond the mean due to asymmetries, overtopping, and the addition of younger understory cohorts, the measured values of θ and b (using the above equations and the simulated data) remain quite good (actual θ: 1.4; measured θ: 1.55; actual, $b = 2.4$; measured, $b = 2.37$).

It was our goal to use only monospecific, closed-canopy, even-aged stands from the Cannell data set. We excluded data from all stands composed of more than one species. We excluded data from stands younger than 30 years, a conservative window to allow canopy closure, and from stands with no recorded age information, which would suggest that they were perhaps not even aged. That still left 220 stands with information on n and D with which to estimate θ (fig. A1*A*) and 81 stands with additional information on B_T with which to estimate b (fig. A1*B*).

We are less concerned with the actual values of the parameters θ and b from the Cannell (1982) data set, which are slightly higher than those used for the numerical work in our model (table A1). Rather, the point is that $\theta \approx b - 1$ (table A1), which justifies our method of reconciling the carbon budget and stem diameter growth in a way that makes diameter growth independent of diameter, as it appears to be for all stems greater than approximately 10 cm DBH (J. Lichstein, personal communication).

We choose our values of θ and b based on the individual-based mass allometries of Jenkins et al. (2003) and Lambert et al. (2005). Their values ($b = 2.43$ for hard maple/oak/hickory/beech species in the United States and $b = 2.37$ for all hardwood species in Canada, respectively) are based on mass measurements of individual trees, which are free from the complications of stand-level averaging described above. Given these methodologically unassailable estimates of b, we back calculate to estimate $\theta = b - 1 \approx 1.4$.

Crown Area and Fine Root Investment

In this section, we demonstrate that the exponent θ, which relates individual crown area to stem diameter is approximately equal to the exponent φ, which relates individual fine root investment to stem diameter. There is very little empirical evidence that relates stem diameter to fine root mass for individual trees in closed-canopy forests. LeGoff and Ottorini (2001) excavated 16 beech trees of widely varying diameters, carefully measuring total fine roots and using allometric equations to estimate missing fine root mass from the diameter of broken coarse roots. The results of this painstaking study suggest an allometric exponent of 2.16 for stem diameter on individual fine root mass. Chen et al. (2004) compiled literature data that were mostly collected at the stand level and related them to individual tree diameters. For various types of cool temperate and boreal forests, their analysis suggests allometric exponents between 1.74 and 2.12 for stem diameter on individual fine root mass.

To our knowledge, no other individual-based fine root estimates for forest trees have been reported. The exponents of LeGoff and Ottorini (2001) and Chen et al. (2004), which we will call φ, are somewhere between the mean of the exponent that relates stem diameter to crown area ($\theta \sim 1.4$) and the mean of the exponent that relates stem diameter to mass ($b \sim 2.4$). We do not know the exact value of θ for the forests from which the authors estimated φ; φ may be greater than, equal to, or less than their particular values of θ. Nevertheless, restricting the Cannell data set to forests composed of beech (*Fagus*) yields an estimated θ, 2.05 (1.80, 2.29), $R^2 = 0.945$, $n = 20$, that encompasses LeGoff and Ottorini's (2001) measured φ value of 2.16 (95% confidence interval in parentheses). With the exception of broadleaf species, subsets of the Cannell data set are similarly consistent with Chen et al. (2004): *Picea*, Chen et al.: 2.12, Cannell: 1.84 (1.39, 2.29), $R^2 = 0.749$, $n = 26$; *Pinus*, Chen et al.: 1.74, Cannell: 1.66 (1.39, 1.94), $R^2 = 0.772$, $n = 46$; *Abies*, Chen et al.: 1.85, Cannell: 1.77 (1.59, 1.94), $R^2 = 0.966$, $n = 18$; and broadleaf, Chen et al.: 1.96, Cannell: 1.70 (1.49, 1.91), $R^2 = 0.749$, $n = 52$.

If φ is significantly different from θ, then our carbon budgets will be incorrect because root diameter will not scale with crown area, meaning that as trees get larger, they will have proportionately more or fewer fine roots per unit crown area than they did when they were smaller. Here, we present a simple mathematical description of a chronosequence undergoing self-cthinning, where we assume three different values of φ, one less than, one greater than, and one equal to θ. Comparing the model output to real chronosequences from the FLUXNET database (Luyssaert et al. 2007) suggests that the real values of φ are indistinguishable from the real values of θ.

We begin by arbitrarily assuming that canopy tree diameters grow 0.5 cm per year and that stem diameters are 0 at the beginning of succession (fig. A2*A*, A2*B*; this choice has no effect on the interpretation). Individual crown area grows as the θ power of diameter. Because $\theta > 1$, there is room for fewer and fewer individuals in the canopy as stem diameters increase; that is, each individual takes up a greater fraction of the total canopy area. This describes the process of self-thinning. We thus determine stand density $n(t)$ by calculating the number of individuals that can fit in the habitat area, T, given individual crown areas (fig. A2*C*, A2*D*):

$$n(t) = \frac{T}{A(D(t))} = \frac{T}{\pi\alpha^{\theta}D^{\theta}(t)}. \tag{A4}$$

For larger θ, fewer individuals can fit for a given stem diameter (cf. fig. A2*C*, A2*D*). Next, we calculate the total fine root mass of the stand by multiplying the total number of individuals by each individual's predicted fine root mass, using allometries presented in appendix G:

$$\sum_{j=1}^{n} Q_{\mathrm{C,r},j}(D(t)) = n(t)Q_{\mathrm{C,r}}(D(t)) = n(t)R_{\mathrm{C,r}}\pi\alpha^{\varphi}D^{\varphi}(t), \tag{A5}$$

where Q is total individual fine root mass (not per area). We arbitrarily choose $R_{\mathrm{C,r}} = 400$ g m^{-2} for the model (this choice has no effect on the interpretation). Substituting $n(t)$,

$$\sum_{j=1}^{n} Q_{\mathrm{C,r},j}(D(t)) = TR_{\mathrm{C,r}}\frac{\pi\alpha^{\varphi}D^{\varphi}(t)}{\pi\alpha^{\theta}D^{\theta}(t)}, \tag{A6}$$

which becomes independent of $D(t)$ and thus t when $\varphi = \theta$. Finally, we express fine root mass on a per-area basis by dividing the left-hand side by T. Results from this simple model are shown in figure A2. Their salient features are the linear increase in stem diameter, the log-log decrease in density that comes as a result of the thinning process, and the dependence of fine root mass on φ relative to θ (and not on the absolute value of φ).

We compared the model output (fig. A2) to the three successional chronosequences with diameter, density, and fine root measurements contained in the FLUXNET data set (Luyssaert et al. 2007) described in appendix D: Andrews Experimental Forest, Cascade Head Experimental Forest, and the University of Michigan Biological Station. The only other site that had more than three data points with all of these measurements was Metolius Research Natural Area, which showed markedly more scatter than the other three sites and an increase in stand density with site age (instead of the decrease expected as a result of self-thinning). It was thus omitted. As in the model, the data show a linear increase in DBH with stand age (fig. A3*A*–A3*C*) and a log-log decrease in density (fig. A3*D*–A3*F*).

Critically, neither fine root net primary productivity (fig. A3*G*–A3*I*) nor fine root mass (fig. A3*J*, A3*K*) vary significantly along the chronosequence (and thus not with mean DBH), consistent with the model prediction that $\varphi = \theta$, or nearly so. Tateno et al. (2009) found a similar result in a *Cryptomeria japonica* plantation chronosequence. We take this as the best evidence available that fine root investment scales with stem diameter just as crown area scales with stem diameter.

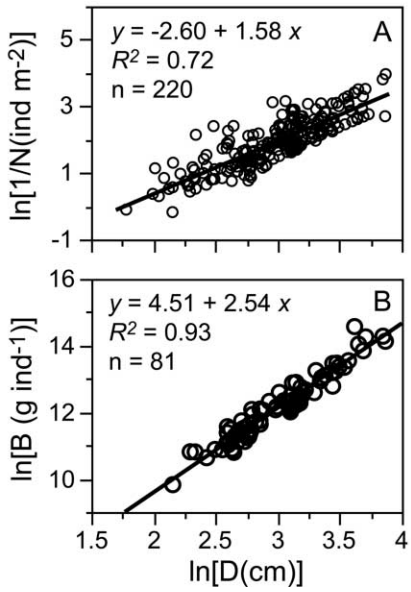

Figure A1: Regression to estimate θ (*A*) and b (*B*) from the Cannell (1982) data set.

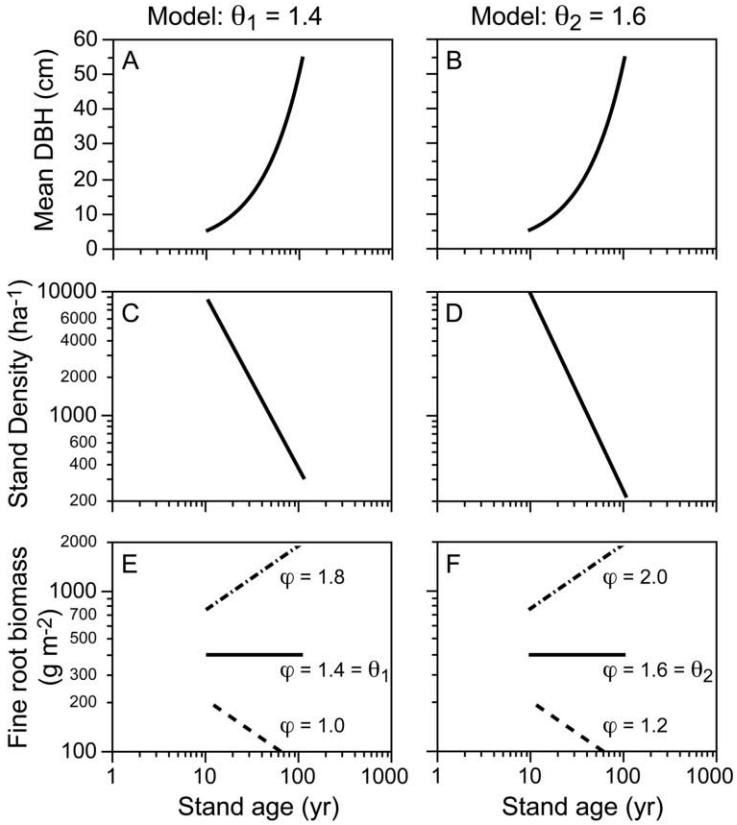

Figure A2: Model (described in text) results for two values of θ (the exponent that relates crown area to stem diameter) and three values of φ (the exponent that relates fine root investment to stem diameter). The critical result is that stand-level fine root mass (*E*, *F*) is predicted to be independent of stand age (and hence mean diameter at breast height [DBH]) when $\varphi = \theta$, whatever the value of θ.

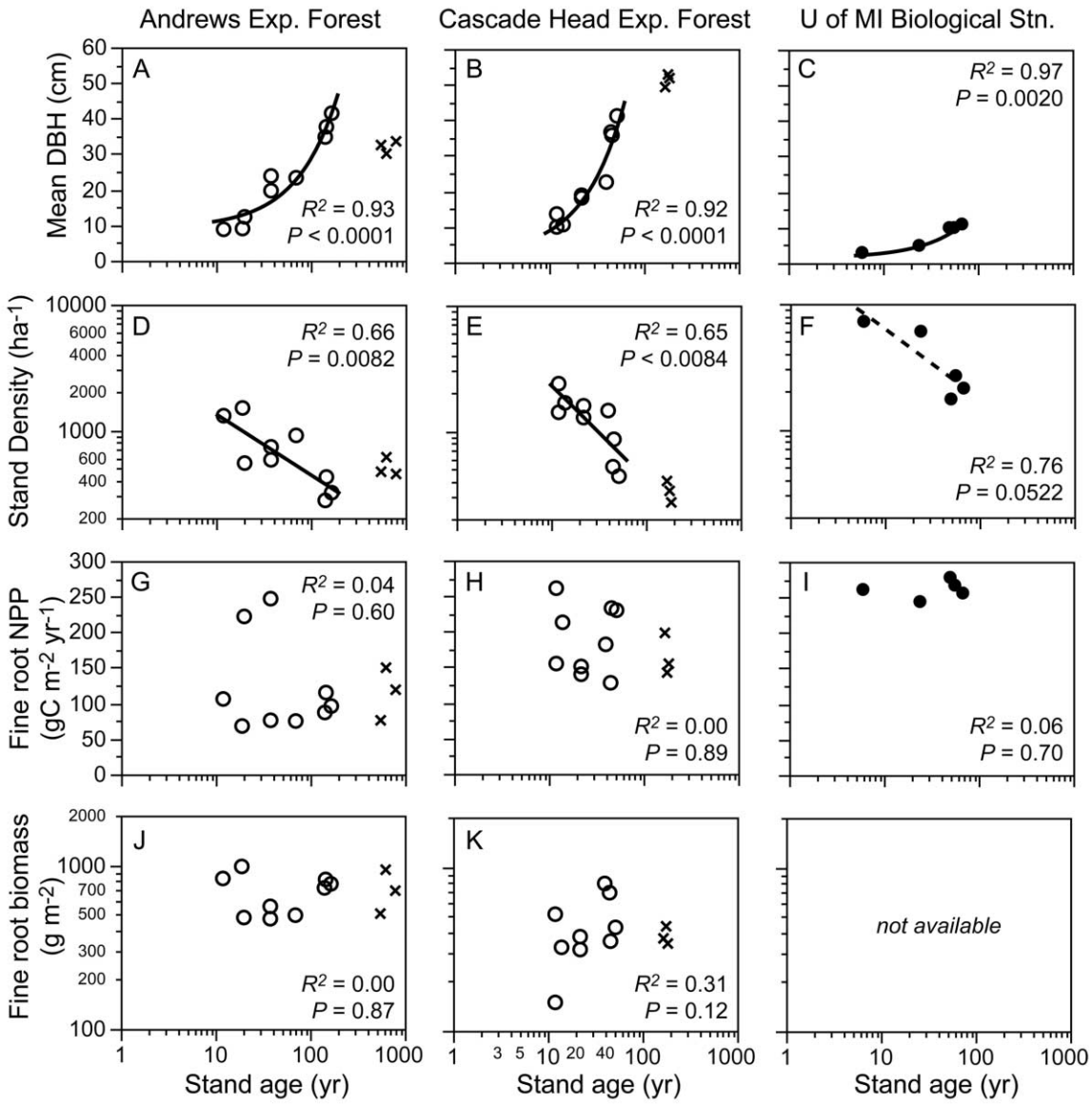

Figure A3: Comparison of aboveground stand characteristics (*top two rows*) to stand-level fine root net primary productivity (NPP) and mass (*bottom two rows*) across three chronosequences (vertically arrayed) in the FLUXNET database (Luyssaert et al. 2007) described in appendix D. Open circles represent stands dominated by gymnosperms; filled circles represent stands dominated by angiosperms; Xs represent old-growth stands dominated by gymnosperms and are omitted from statistical fits. As predicted by the model (fig. A2), fits are mean diameter at breast height: linear; stand density: log-log; fine root NPP: log-log; and fine root mass: log-log. *Solid lines* = statistically significant fits; *dashed lines* = fits that are not significant two-tailed tests but are significant one-tailed tests; and *no lines* = nonsignificant fits. Note goofy smiley face in *G*.

Additional Literature Cited in Appendix A

Cannell, M. G. R. 1982. World forest biomass and primary production data. Academic Press, London.

Chen, W. J., Q. F. Zhang, J. Cihlar, J. Bauhus, and D. T. Price. 2004. Estimating fine-root biomass and production of boreal and cool temperate forests using aboveground measurements: a new approach. Plant and Soil 265:31–46.

Jenkins, J. C., D. C. Chojnacky, L. S. Heath, and R. A. Birdsey. 2003. National-scale biomass estimators for United States tree species. Forest Science 49:12–35.

Lambert, M. C., C. H. Ung, and F. Raulier. 2005. Canadian national tree aboveground biomass equations. Canadian Journal of Forest Research 35:1996–2018.

Le Goff, N., and J. M. Ottorini. 2001. Root biomass and biomass increment in a beech (*Fagus sylvatica* L.) stand in north-east France. Annals of Forest Science 58:1–13.

Tateno, R., K. Fukushima, R. Fujimaki, T. Shimamura, M. Ohgi, H. Arai, N. Ohte, et al. 2009. Biomass allocation and nitrogen limitation in a *Cryptomeria japonica* plantation chronosequence. Journal of Forest Research 14: 276–285.

 DOI: 10.1086/657992

Appendix B from R. Dybzinski et al., "Evolutionarily Stable Strategy Carbon Allocation to Foliage, Wood, and Fine Roots in Trees Competing for Light and Nitrogen: An Analytically Tractable, Individual-Based Model and Quantitative Comparisons to Data"

(Am. Nat., vol. 177, no. 2, p. 153)

Comparison of Full Carbon Budget Accounting to Simplifications

Here, we compare two methods of carbon accounting for a single tree growing from seed in the understory through 77 years in the canopy. Both methods keep track of carbon on a monthly basis, ignoring dormant periods. Given a complement of foliage, the tree fixes carbon and respires, given its light regime. It allocates carbon for the build of foliage and fine roots, along with fine root respiration, and senesces some fraction of those organs. At the beginning of the next month, it assesses its foliage and fine root complement. It allocates carbon to meet its target foliage $L_{X,r}$ first, followed by target fine root mass $R_{X,r}$ and target fecundity ω_C (only if it is in the canopy), with whatever remains going to wood increment.

In the first method, "full," the tree must allocate carbon to the new annulus of leaves and fine roots that come with each new increment of wood growth (and hence crown area increment), as real trees must. Moreover, when it transitions from the understory to the canopy, it must allocate carbon to increase $L_{U,r}$ and $R_{U,r}$ to $L_{C,r}$ and $R_{C,r}$, as real trees must. In contrast, the second method, "simplified," allows trees to add an annulus of leaves and fine roots at no cost, and allows trees to increase $L_{U,r}$ and $R_{U,r}$ to $L_{C,r}$ and $R_{C,r}$ instantaneously and at no cost when they transition to the canopy. The simplified method is exactly the method used in main text of this article. The purpose of this appendix is to demonstrate that its simplifications result in only small differences in understory survivorship and lifetime fecundity.

For both methods, we use L_C^*, L_U^*, R_C^*, and R_U^* as the target values across an N_{avail} gradient. For the simplified method, we use $\tilde{D}_r$ values to separate understory from canopy growth. For the full methods, we initially use this same value of $\tilde{D}_r$, which will be close to correct, and then take the average understory and canopy growth rates to calculate a more accurate value of $\tilde{D}_r$, using the equation found in appendix G. We then use this second, more accurate, value of $\tilde{D}_r$ to separate understory from canopy growth in the final result. As in the main text, we use an understory mortality rate of 0.038 per year. Thus the understory tree has a 96.2% chance of surviving from one year to the next. We calculate survivorship as 0.962 raised to the number of years spent in the understory. As in the model presented in the main text, fecundity is proportional to crown area. Thus, a faster-growing tree will have greater lifetime fecundity than a slower-growing tree, assuming, as we do in this appendix, that they both die after 77 years in the canopy.

A comparison of understory and canopy growth rates together with their resulting $\tilde{D}_r$ are shown in figure B1. Understory growth rates in the full method are always less than in the simplified method because the annulus of leaves and fine roots that it includes (and the simplified method ignores) is a significant fraction of total crown volume for small-diameter trees. For the same reason, full method canopy growth rates are always less than those of the simplified method, though the annulus effect becomes less important for larger trees as the volume of the annulus becomes a smaller fraction of the total canopy volume. As a result of these shifts in understory and canopy growth rates, the $\tilde{D}_r$ values of the full method are always lower than they are in the simplified method (fig. B1*C*).

Survivorship in the understory (fig. B2*A*) is similar for both methods across most of the N_{avail} gradient, with median values for the full method less than 6% different than the values for the simplified method survivorship. Lifetime fecundity is similar for both methods across most of the N_{avail} gradient (fig. B2*C*), with median values for the full method less than 15% different from the simplified method lifetime fecundity. The differences in survivorship and fecundity between the methods are greatest at low N_{avail} and diminish to almost nothing at high

N_{avail}. Moreover, the two effects work in opposition to diminish their cumulative effect on lifetime reproductive success: the full method results in a greater fraction of understory individuals surviving to the canopy but fewer offspring created once in the canopy. The transition time from L_{U} to L_{C} is at most 3 months (fig. B2*B*), suggesting that the simplified method, which assumes that the transition is costless and instantaneous, is a reasonable approximation for trees that live on the order of 77 years. Overall, we conclude that our simplified method, which generates precisely the same growth rates as the model presented in the main body of this article, is a reasonable approximation of that more realistic but less tractable method.

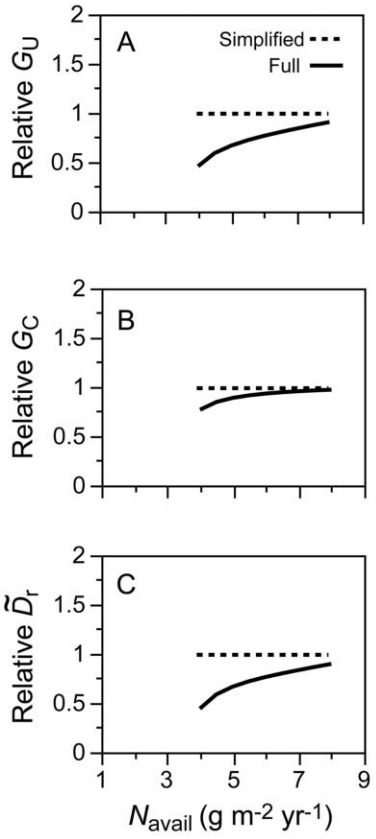

Figure B1: Comparison of simplified and full methods of individual tree carbon budgeting (see app. B text for explanation of method differences) on growth rates (*A*, *B*) and $\tilde{D}_{\text{r}}$ (*C*). All values are normalized by the simplified method's values.

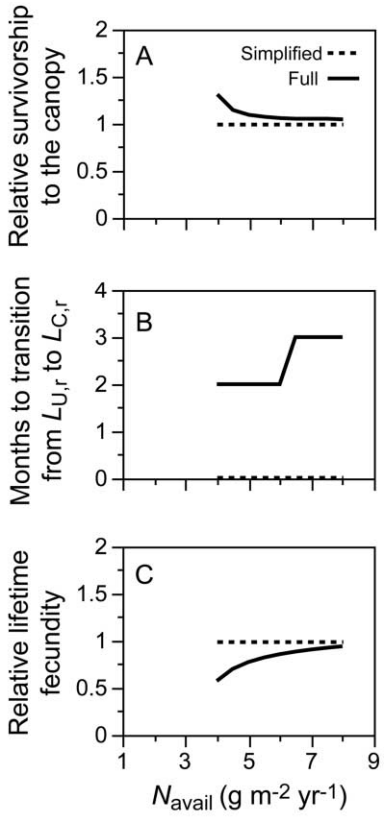

Figure B2: Comparison of simplified and full methods of individual tree carbon budgeting (see app. B text for explanation of method differences) on understory survivorship (*A*), transition time to canopy $L_{C,r}$ (*B*), and lifetime fecundity (*C*). Except for *B*, all values are normalized by the simplified method's values.

 DOI: 10.1086/657992

Appendix C from R. Dybzinski et al., "Evolutionarily Stable Strategy Carbon Allocation to Foliage, Wood, and Fine Roots in Trees Competing for Light and Nitrogen: An Analytically Tractable, Individual-Based Model and Quantitative Comparisons to Data"

(Am. Nat., vol. 177, no. 2, p. 153)

Open-Canopy Conditions

Depending on the values of $R_{X,x}$, $L_{X,x}$, $G_{X,x}$, N_{avail}, and other parameters, a stable equilibrium monoculture may either have an open canopy, with $\tilde{Z}_r = 0$ and all individuals in full sun, or a closed canopy, with $\tilde{Z}_r > 0$ and individuals germinating in the shade. Strigul et. al. (2008) show that a closed-canopy equilibrium is locally stable, if it exists, for reasonable parameter values.

R_{open}: Transition between Open Canopy and Closed Canopy

The transition from equilibrial open-canopy forest to equilibrial closed-canopy forest will occur wherever $\tilde{Z}_r$ (or equivalently $\tilde{D}_r$ if we assume the same height-diameter relations among all strategies, as we do in this article) is equal to 0 (such that there is no understory stage) and each individual is just able to replace itself in a lifetime spent in the "canopy," such that the total crown area exactly fills the habitat; that is, $\sum A(D) = T$. This transition can be found by solving the following expression (derived from eq. [10]) for R_{open}, assuming an $L_{C,r} = L_C^*$ that is not nitrogen saturated:

$$W_r = 1 = F\pi\alpha^\theta\Gamma(\theta + 1)\frac{G_{C,r}^\theta(R_{open})}{\mu_C^{\theta+1}}, \tag{C1}$$

where $G_{C,r}$ is a function of R_{open}. When canopy photosynthesis is light saturated (eq. [5]), R_{open} is a linearly increasing function of N_{avail}:

$$R_{open} = \frac{[sA_{max} - \gamma_L M(1 + \kappa_L)]L_C^* - \omega_C - \mu_C^{(\theta+1)/\theta}c_1}{\gamma_R(1 + \kappa_R) + \Omega}, \tag{C2}$$

where

$$c_1 = \frac{a(\theta + 1)}{\pi\alpha^\theta}[F\pi\Gamma(\theta + 1)]^{-1/\theta} \tag{C3}$$

and L_C^* is an increasing function of N_{avail} as given by equation (14). When canopy photosynthesis is dual limited (eq. [6]), R_{open} is an increasing but saturating function of N_{avail}:

$$R_{open} = \frac{s\left\{\frac{A_{max}+q}{k}\left[1 + \ln\left(\frac{\Phi I_C^0}{A_{max}+q}\right)\right] - \frac{\Phi I_C^0}{k}e^{-kL_C^*}\right\} - [sq + \gamma_L M(1 + \kappa_L)]L_C^* - \omega_C - \mu_C^{(\theta+1)/\theta}c_1}{\gamma_R(1 + \kappa_R) + \Omega}. \tag{C4}$$

For a given N_{avail}, all $R_{C,r} > R_{open}$ will form open-canopy stands, whereas all $R_{C,r} \le R_{open}$ will form closed-canopy stands.

There Is No Closed-Canopy R_C^* in Which the Resident Canopy Is Solely Nitrogen Limited

If we attempt to solve the ESS condition (eq. [11]) using the simplified carbon conservation equation (eq. [8]) together with net photosynthesis for a solely light-limited canopy (eq. [5]), we find that

$$R_C^* = \frac{[sA_{max} - \gamma_L M(1 + \kappa_L)]L_C^*}{\gamma_R(1 + \kappa_R) + \Omega}. \tag{C5}$$

But inspection of both this equation and the equation for R_{open} in the solely nitrogen-limited case (eq. [C2]) reveals that $R_C^* > R_{open}$. Thus, R_C^* cannot sustain a closed-canopy forest. This derivation is sufficient to show that there can be no ESS closed-canopy forest when the canopy is solely nitrogen limited, but it does not result in a valid expression for R_C^* in this case. Our derivations of both $N_{X,x}$ and W_x assumed a closed canopy (app. G) and, as such, are no longer valid in the open-canopy case. A complete analysis of the open-canopy case is beyond the scope of this article.

 DOI: 10.1086/657992

Appendix D from R. Dybzinski et al., "Evolutionarily Stable Strategy Carbon Allocation to Foliage, Wood, and Fine Roots in Trees Competing for Light and Nitrogen: An Analytically Tractable, Individual-Based Model and Quantitative Comparisons to Data"

(Am. Nat., vol. 177, no. 2, p. 153)

Description of Allocation Data Assembled from FLUXNET

FLUXNET Database

The FLUXNET study draws from data that have been collected at a large number of sites ($n > 400$) around the world where net ecosystem exchange (NEE) of CO_2 between the terrestrial biosphere and the atmosphere has been measured extensively and pooled to permit synthesis activities as part of the FLUXNET program (Baldocchi et al. 2001; Baldocchi and Valentini 2004; Luyssaert et al. 2007). A subset of these sites was summarized in a database presented by Luyssaert et al. (2007) that compiled component flux data from sites, wherever available, on annual net primary productivity (NPP) separated by foliage, branch, stem, coarse roots, and fine roots. The NPP of these components includes growth that was subsequently lost to mortality (e.g., litterfall) but is the net of carbon respired in growth and maintenance, such that summing component NPP and ecosystem respiration should in principle equal the NEE measured by eddy covariance; the closure between bottom-up and top-down estimates is generally within 5%. Because the Luyssaert database is compiled from a large number of studies, methods employed to estimate component NPP vary between sites, and not all components are available for all sites. Nevertheless, the Luyssaert database is incomparable for compiling estimates of NEE at different hierarchical levels (aboveground NPP, belowground NPP, ecosystem respiration, herbivory, non-CO_2 carbon emission, leaching) and among different sites and years to analyze biotic and abiotic controls on NEE across ecosystems globally (e.g., Luyssaert et al. 2007).

For the purposes of this article, we include only sites where all components of NPP (foliage, branch, stem, coarse root, fine root) are reported and where the methodology for measuring each is known ($n = 139$). Fractional allocation to foliage was calculated as foliage NPP divided by total NPP (foliage + branch + stem + coarse root + fine root). Fractional allocation to aboveground wood was calculated as branch + stem NPP divided by total NPP. Fractional allocation to fine root was calculated as fine root NPP divided by total NPP. Absolute allocation to foliage and fine roots is simply the reported values. Absolute allocation to aboveground wood is the sum of branch NPP + stem NPP.

Among the usable sites, 40 are dominated by angiosperms (*filled circles* in figures), and 99 are dominated by gymnosperms (*open circles* in figures). The sites are generally located at temperate ($n = 88$) and boreal ($n = 45$) regions, with few in tropical ($n = 5$) and Mediterranean ($n = 1$) regions. Figure D1 breaks the fractional NPP figures of the main text by temperate and boreal stands, revealing that, apart from the lower absolute total NPP of the boreal sites, the general patterns are shared by both. The sites were given a variety of codes to characterize management of the stands; most stands were managed forests ($n = 62$), many were natural forests ($n = 34$), some were categorized as recently disturbed ($n = 24$), a small number were given fertilizer or irrigation ($n = 9$), and for some no information was available ($n = 10$). Figure D2 classifies the fractional NPP figures of the main text by management status, revealing that the general patterns are shared by them all.

A range of techniques were employed to measure fine root NPP, including "higher-quality" measurements of biomass and in situ turnover using minirhizotrons or root windows ($n = 56$), "modest-quality" techniques such as biomass with an assumed turnover rate ($n = 45$) or root ingrowth techniques ($n = 5$), and "lower-quality" techniques based on sequential coring ($n = 27$). Some sites used techniques for fine root growth that were ambiguous from the study text ($n = 6$), which we conservatively lump with the "lower-quality" techniques.

Figure D3 classifies the fractional NPP figures of the main text by fine root NPP measurement technique, revealing that the general patterns are recovered using any of these methods. The vast majority of studies to estimate coarse root NPP were derived from allometric considerations ($n = 104$), with the remaining sites deriving coarse root NPP from biomass and in situ turnover observations ($n = 10$), ingrowth techniques ($n = 4$), and sequential coring ($n = 18$), as well as from some sites with ambiguous methodology ($n = 5$). Readers are encouraged to refer to Luyssaert et al. (2007) for more detail on the methods used to compile the data hierarchically, as well as for citations to the original data comprising the database.

To the FLUXNET data, we added 13 additional data points originally collected by Santantonio (1989) for exactly the same analysis performed here. All 13 stands are dominated by gymnosperms in temperate latitudes. Given their vintage, estimates of fine root NPP were likely done with a sequential coring technique, which is what we assume here.

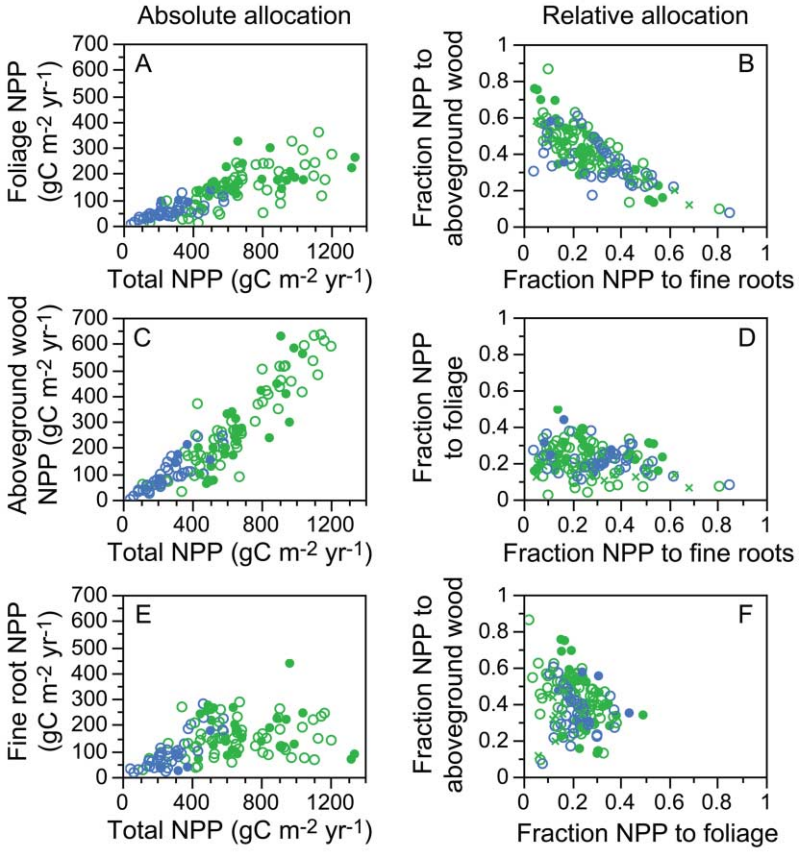

Figure D1: Relations between the net primary productivity (NPP) allocated to foliage, fine roots, and aboveground wood separated by boreal forest (*blue*) and temperate forest (*green*). Circles represent data from the publicly available FLUXNET database (Luyssaert et al. 2007) and Xs represent data from Santantonio (1989). Stands represented by open circles or Xs are dominated by gymnosperms, whereas those represented by filled circles are dominated by angiosperms.

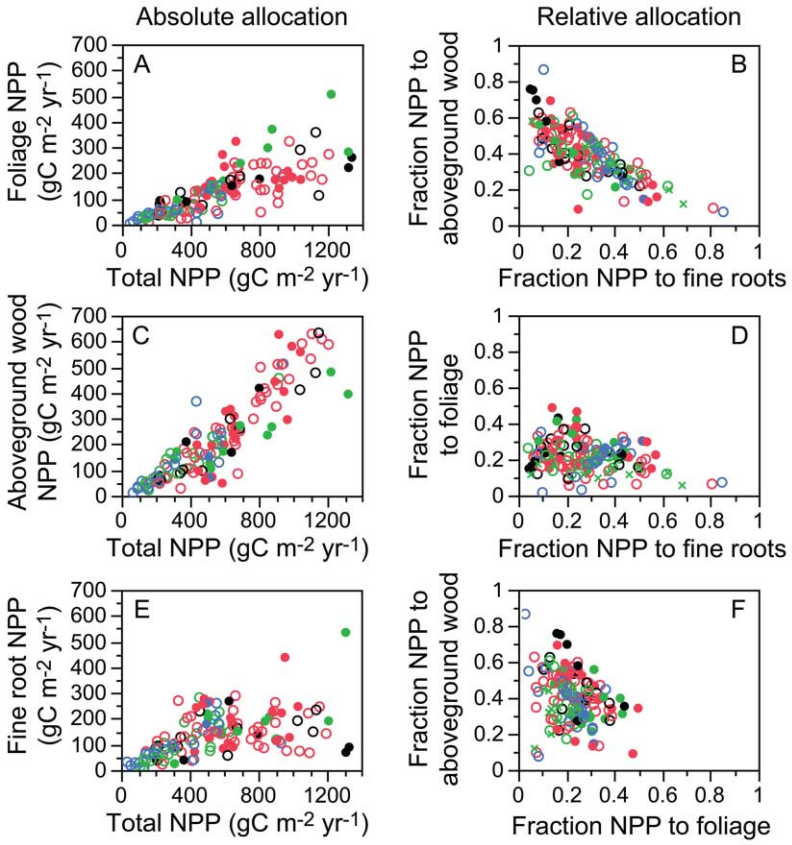

Figure D2: Relations between the net primary productivity (NPP) allocated to foliage, fine roots, and aboveground wood separated by the management status of stands: *red* = managed; *green* = unmanaged; *blue* = recently disturbed; *black* = other. Circles represent data from the publicly available FLUXNET database (Luyssaert et al. 2007) and Xs represent data from Santantonio (1989). Stands represented by open circles or Xs are dominated by gymnosperms, whereas those represented by filled circles are dominated by angiosperms.

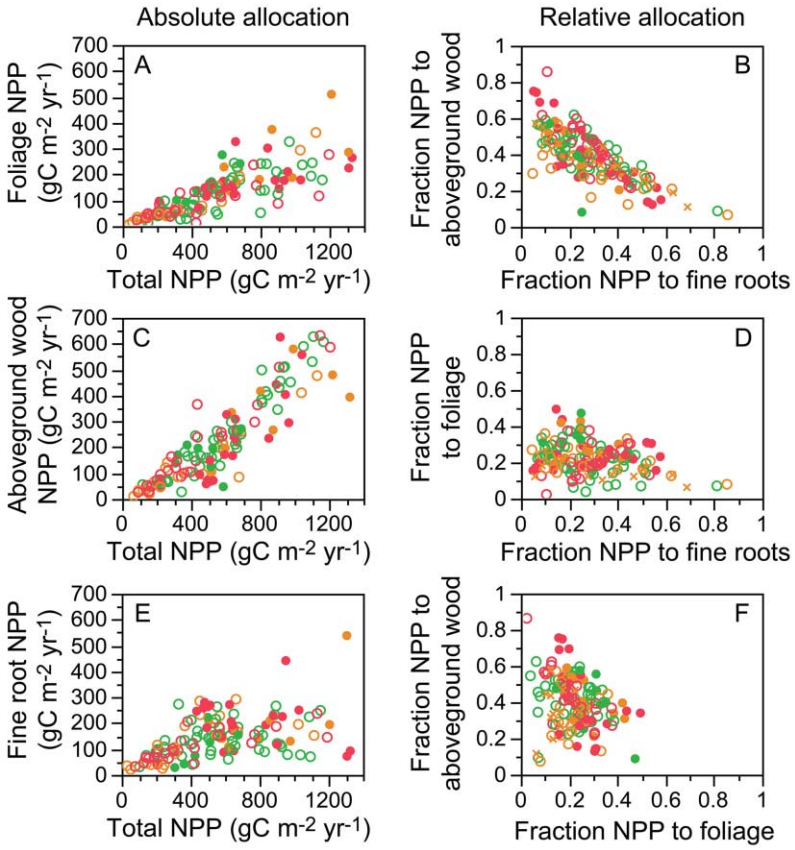

Figure D3: Relations between the fraction of net primary productivity (NPP) allocated to foliage, fine roots, and aboveground wood separated by method of estimating fine root NPP: *green* = higher quality; *orange* = modest quality; *red* = low quality (see text for details). Circles represent data from the publicly available FLUXNET database (Luyssaert et al. 2007) and Xs represent data from Santantonio (1989). Stands represented by open circles or Xs are dominated by gymnosperms, whereas those represented by filled circles are dominated by angiosperms.

Additional Literature Cited in Appendix D

Baldocchi, D., and R. Valentini. 2004. Geographic and temporal variation of carbon exchange by ecosystems and their sensitivity to environmental perturbations. Pages 295–316 *in* C. B. Field and M. R. Raupach, eds. The global carbon cycle: integrating humans, climate and the natural world. Island, Washington, DC.

Baldocchi, D., E. Falge, L. H. Gu, R. Olson, D. Hollinger, S. Running, P. Anthoni, et al. 2001. FLUXNET: a new tool to study the temporal and spatial variability of ecosystem-scale carbon dioxide, water vapor, and energy flux densities. Bulletin of the American Meteorological Society 82:2415–2434.

 DOI: 10.1086/657992

Appendix E from R. Dybzinski et al., "Evolutionarily Stable Strategy Carbon Allocation to Foliage, Wood, and Fine Roots in Trees Competing for Light and Nitrogen: An Analytically Tractable, Individual-Based Model and Quantitative Comparisons to Data"

(Am. Nat., vol. 177, no. 2, p. 153)

Parameter Value Sources and Derivations

We assign values to our parameters for the purposes of creating figures and comparing our model predictions to data. We report the sources and derivations of those values here.

Table E1. Parameter value sources and derivations

Symbol	Value	Units	Description	Source
Allometric equations:				
α	.1	$m^{2/\theta}$ cm	Power law coefficient relating D to A	Purves et al. 2008, their appendix A1; values estimated from Forest Inventory Analysis data for forests in the Great Lakes states region of the United States; approximate values for *Acer rubrum* across all soil types
θ	1.4	None	Power law exponent relating D to A; calculated as one less than the value of b (see app. A)	
φ	1.4	None	Power law exponent relating D to $R_{X,x}$; calculated as one less than the value of b (see app. A)	

Table E1 (*Continued*)

Symbol	Value	Units	Description	Source
a	81.5	$g_{carbon}\ cm^{-(\theta+1)}$	Power law coefficient relating D to B. Jenkins et al. estimated the power law relationship between DBH and aboveground biomass for North American tree species. Taking the mean value for "hard maple/oak/hickory/beech" (their table 4) and converting to unexponentiated form and grams gives 133.6 $g_{biomass}\ cm^{-(\theta+1)}$. Because we are also interested in including structural belowground biomass in our model, we use results from White et al. for deciduous broadleaf forests: aboveground wood represents .78 of total wood production. Thus, we multiply Jenkins et al.'s value by $1 + (1 - .78) = 1.22$ and divide by 2 to approximate grams carbon (instead of biomass) in coarse roots, root crowns, stems, and branches.	Jenkins et al. 2003; White et al. 2000, sec. A.2.4
b	2.4	None	Power law exponent relating D to B	Jenkins et al. 2003, "hard maple/oak/hickory/beech," their table 4
h	3.58	$m\ cm^{-\beta}$	Power law coefficient relating D to H	Purves et al. 2008, their appendix A1; values estimated from Forest Inventory Analysis data for forests in the Great Lakes states region of the United States; approximate values for *A. rubrum* across all soil types
β	.5	None	Power law exponent relating D to H	Purves et al. 2008, their appendix A1; values estimated from Forest Inventory Analysis data for forests in the Great Lakes states region of the United States; approximate values for *A. rubrum* across all soil types
Nitrogen:				
ρ	.5	None	Fraction of total plant nitrogen uptake allocated to leaves; nitrogen lost in leaf litter (3.36 $g\ m^{-2}\ year^{-1}$) plus nitrogen lost in leaf leaching (.99 $g\ m^{-2}\ year^{-1}$) divided by total plant uptake (8.82 $g\ m^{-2}\ year^{-1}$) $\approx .5$	From Whittaker et al. 1979, their table 5
δ_L	1.595	$g_N\ m^{-2}$	Nitrogen per unit leaf area; average value for trees that are from the temperate forest biome, deciduous, broadleaf, and non-N-fixing	Average value taken from GLOPNET database; Wright et al. 2004
f	.5	None	Fraction of nitrogen lost from senesced foliage; roughly half of nitrogen is lost from senescing leaves	
γ_L	1	$year^{-1}$	Foliage turnover; we model deciduous trees	
Light and photosynthesis:				
A_{max}	9.9×10^{-5}	$g_{carbon}\ LAI^{-1}\ m^{-2}\ s^{-1}$	Maximum net carbon assimilation rate (see fig. 2); average value for *A. rubrum*	Average value taken from GLOPNET database; Wright et al. 2004
q	9.9×10^{-6}	$g_{carbon}\ LAI^{-1}\ m^{-2}\ s^{-1}$	Dark respiration rate (see fig. 2); one-tenth A_{max}, the approximate relationship between q and A_{max} for trees in the GLOPNET database	GLOPNET database; Wright et al. 2004
Φ	3.27×10^{-4}	$g_{carbon}\ LAI^{-1}\ m^{-2}\ s^{-1}\ PAR^{-1}\ PAR_0$	Quantum yield of light-limited net photosynthesis (see fig. 2); calculated from A_{max} and q assuming leaves become light limited at one-third full sunlight	Barbour et al. 1987, p. 426, "sun adapted leaves of C3 plants"

Table E1 (*Continued*)

Symbol	Value	Units	Description	Source
s	2.26×10^6	s year^{-1}	Scale conversion between measured (s^{-1}) and yearly net photosynthesis. Because a "bottom-up" approach would be subject to too many multiplicative errors and poorly understood factors, we take a "top-down" approach to calculate s. Assuming a nitrogen-rich temperate forest has a total (aboveground + belowground) NPP ~825 g_{carbon} m^{-2} year^{-1}, we use the expression in the main text for dual limited net carbon gain ($E_{C,r}$) together with the values in this table for k, I_C^0, A_{max}, q, Φ, and an assumed LAI of 6 to solve for s.	
k	.5	LAI^{-1}	Light extinction coefficient per crown depth	White et al. 2000, sec. A.7.2
ζ	.75	None	Scales k and $L_{C,r}$ in Beer's law light extinction to calculate I_U^0; estimated value arrived at by comparing understory growth rates to those of Purves et al.	Purves et al. 2008
Carbon:				
M	28	g_{carbon} LAI^{-1} m^{-2}	Leaf carbon per area. The average LMA for trees that are from the temperate forest biome and are deciduous, broadleaved, and non-N-fixing is 37.4; because these are sun leaves, we estimate shade leaves as half this value; we take the average of the sun leaf value and the shade leaf value	Average LMA from GLOPNET database; Wright et al. 2004
κ_L	.25	None	Foliage construction respiration, expressed as a fraction of leaf carbon	Ryan 1991
γ_R	.3	year^{-1}	Fine root turnover. Fine root turnover is notoriously difficult to measure; a value of .3 is not unreasonable and, together with Ω, generates realistic standing fine root biomass	
κ_R	.25	None	Fine root construction respiration, expressed as a fraction of fine root carbon	Ryan 1991
Ω	.35	g_{carbon} g_{carbon}^{-1} year^{-1}	Fine root respiration rate. Estimates of fine root respiration are scarce even on short timescales, let alone extrapolated to an entire growing season; we use a value of .35, which seems reasonable and generates standing fine root biomass, which also seems reasonable	
ω_C	34.6, 0	g_{carbon} m^{-2} year^{-1}	Carbon cost of producing seeds; 0 for understory individuals; Whittaker et al. report NPP of fecundity as ~17.3 g_{carbon} m^{-2} year^{-1}, which we double to approximately account for the respiration of the reproductive structures	Whittaker et al. 1974
Λ	.78	None	Fraction aboveground of the carbon allocated to wood	White et al. 2000, sec. A.2.4 for deciduous broadleaf forests
Perfect plasticity approximation:				
μ_X	.013, .038	year^{-1}	Mortality rate for canopy and understory, respectively	Purves et al. 2008, their appendix A1; values estimated from Forest Inventory Analysis data for forests in the Great Lakes states region of the United States; mean values for angiosperms on mesic soils
F	.01	individuals m^{-2} year^{-1}	Germinants produced per unit canopy area per time	Purves et al. 2008, their appendix A1; values estimated from Forest Inventory Analysis data for forests in the Great Lakes states region of the United States

Note: DBH = diameter at breast height; PAR = photosynthetically active radiation; NPP = net primary productivity; LAI = leaf area per ground area of an individual; LMA = leaf mass per area.

Additional Literature Cited in Appendix E

Barbour, M. G., J. H. Burk, and W. D. Pitts. 1987. Terrestrial plant ecology. Benjamin/Cummings, Menlo Park, CA.

Jenkins, J. C., D. C. Chojnacky, L. S. Heath, and R. A. Birdsey. 2003. National-scale biomass estimators for United States tree species. Forest Science 49:12–35.

Ryan, M. G. 1991. Effects of climate change on plant respiration. Ecological Applications 1:157–167.

White, M. A., P. E. Thornton, S. W. Running, and R. R. Nemani. 2000. Analysis of the BIOME-BGC terrestrial ecosystem model: net primary production controls. Earth Interactions 4:1–85.

Whittaker, R. H., F. H. Bormann, G. E. Likens, and T. G. Siccama. 1974. The Hubbard Brook ecosystem study: forest biomass and production. Ecological Monographs 44:233–254.

Whittaker, R. H., G. E. Likens, F. H. Bormann, J. S. Easton, and T. G. Siccama. 1979. The Hubbard Brook ecosystem study: forest nutrient cycling and element behavior. Ecology 60:203–220.

Wright, I. J., P. B. Reich, M. Westoby, D. D. Ackerly, Z. Baruch, F. Bongers, J. Cavender-Bares, et al. 2004. The worldwide leaf economics spectrum. Nature 428:821–827.

 DOI: 10.1086/657992

Appendix F from R. Dybzinski et al., "Evolutionarily Stable Strategy Carbon Allocation to Foliage, Wood, and Fine Roots in Trees Competing for Light and Nitrogen: An Analytically Tractable, Individual-Based Model and Quantitative Comparisons to Data"

(Am. Nat., vol. 177, no. 2, p. 153)

Graphical Global Adaptive Dynamics Analyses

The evolutionarily stable strategy (ESS) calculations presented in the main text find singular strategies that cannot be invaded by nearby strategies. However, it is possible that these singular strategies might be invasible by very different strategies or may be unattainable by successive invasions from some starting conditions. Here, we plot pairwise invasibility for fine root allocation to determine whether the ESSs calculated in the main text are global (i.e., uninvasible not just by nearby strategies but by any strategy) and convergent stable (i.e., attainable by successive invasion from any starting resident strategy). That the ESS allocation to foliage is both global and convergence stable follows as a consequence of its optimality (see "Result 5" in app. G).

We created pairwise invasibility plots of fine root allocation by allowing all possible invader strategies to invade all possible resident strategies, highlighting those combinations that yield successful invasion. We calculated the canopy pairwise invasibility assuming the understory individuals of both resident and invader played the best strategy for the conditions created by the resident. We calculated the understory pairwise invasibility assuming the canopy individuals of both resident and invader played the ESS.

The pairwise invasibility plots reveal that the ESS fine root allocation strategies presented in the main text are both global and convergent stable (fig. F1). Neither canopy nor understory fine root allocation strategies reveal possibilities for coexistence, either involving ESSs or off-ESSs. Understory ESSs will invade any non-ESS. In contrast, the canopy strategies reveal many pairwise interactions that are founder controlled, including those that involve the ESS. A full discussion of the model's founder control is beyond the scope of this article, but we briefly note that there is an "ideal" invasion fine root allocation strategy for any given resident strategy (except the ESS). That ideal invasion strategy maximizes carbon capture in the environment created by the resident. For residents that have a fine root allocation strategy below the ESS, the ideal invasion fine root strategy is greater than the resident's but not too much greater: at some point, greater invader fine root mass is no longer advantageous, as the benefits have saturated (due to self-shading) but the costs keep increasing. Parallel reasoning explains founder control involving resident fine root allocation strategies that are above the ESS.

However, we note that any off-ESS may be invaded by a sufficiently similar strategy, providing a path of successive invasions from any off-ESS to the ESS (i.e., the ESS is convergent stable).

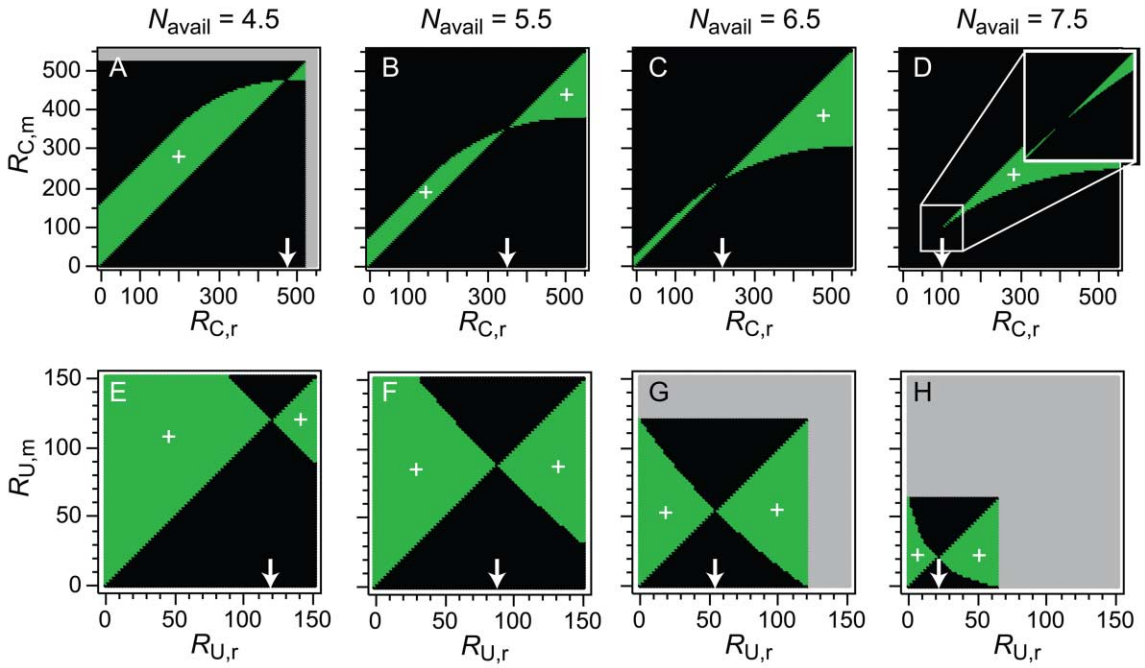

Figure F1: Pairwise invasibility plots of canopy (*A–D*) and understory (*E–H*) fine root allocation. Black areas reveal areas where the invading strategy (*Y*-axis) cannot successfully invade the resident strategy (*X*-axis); green areas (with "+" where space permits) show where the invasion is successful, and gray indicates strategies that do not generate equilibrial closed-canopy forest. The analysis found areas of founder control but no areas of coexistence. The evolutionarily stable strategy is indicated by an arrow. The inset in *D* reveals the ESS in higher resolution ("zooming in" always shows the same qualitative shape as in, e.g., *C*).

 DOI: 10.1086/657992

Appendix G from R. Dybzinski et al., "Evolutionarily Stable Strategy Carbon Allocation to Foliage, Wood, and Fine Roots in Trees Competing for Light and Nitrogen: An Analytically Tractable, Individual-Based Model and Quantitative Comparisons to Data"

(Am. Nat., vol. 177, no. 2, p. 153)

Full Model Derivation and Description and Derivation of Analytical Results

Model Overview

Figure 1 in the main text provides a conceptual depiction of our model. In it, individuals in either a canopy stage or an understory stage compete for nitrogen as a function of their fine root mass. We assume an old-growth monoculture of resident individuals and invader individuals of negligible population density. Because of stoichiometric constraints on the construction of foliage, better competitors for nitrogen are able to build more foliage and worse competitors for nitrogen are able to build less foliage. Given a complement of foliage, individuals photosynthesize. At the top of the canopy, leaves photosynthesize at the maximum rate, but that rate diminishes in lower leaves due to self-shading. In addition to self-shading, the photosynthesis of understory individuals is reduced by the shade of the canopy individuals above them. Individuals allocate fixed carbon to support foliage, fine roots, and, if they are in the canopy, reproductive structures. Whatever carbon remains is allocated to structural wood (branches, stem, and coarse roots), which determines stem diameter growth rate, and, via allometry, height growth rate.

By reasonable approximation, our model predicts two diameter-independent growth rates, one for the canopy and another for the understory (see below for details), which are directly used in the perfect plasticity approximation (PPA) macroscopic equations (Strigul et al. 2008). The PPA scales the individual-level ecology to the community level, where we use adaptive dynamics (McGill and Brown 2007) to determine the most competitive allocations to foliage, wood, and fine roots for a given nitrogen availability. We use the term "strategy" to refer to a particular suite of such allocations. All other resources, including water and phosphorus, are assumed to be nonlimiting regardless of allocation.

We use the terms "nitrogen limited," "light limited," and "dual limited" to reflect their empirical interpretations, where adding nitrogen, light, or either nitrogen or light would increase growth rates, respectively. To be clear, a "dual-limited" individual would benefit from the addition of nitrogen by itself, light by itself, or both together. We use the term "dual limited" and not "colimited" to remain uncommitted as to whether the addition of both nitrogen and light would result in interactive or (merely) additive effects, only the former of which is currently defined as "colimitation" (Harpole and Goldstein 2007).

Nomenclature for Parameters and Subscripts

Table G1 lists all model parameters and variables along with the values used to produce figures. Wherever appropriate, the subscript X is a placeholder and indicates that canopy individuals (subscript C) may have a different value (e.g., $R_{C,x}$) than understory individuals (subscript U; e.g., $R_{U,x}$). The subscript x is also a placeholder and indicates that a resident value (subscript r; e.g., $R_{X,r}$) may differ from an invader value (subscript m; e.g., $R_{X,m}$). Together, we write, for example, $R_{C,r}$ when we specifically refer to the variable R for resident individuals (r) in the canopy stage (C). In contrast, we write $R_{X,x}$ when we generically refer to the variable R for either invaders or residents (x) of either the canopy or understory stages (X). To determine the adaptive dynamics of the system, we assume the resident dominates the habitat and that the population size of the invader is negligible. Thus, the resident affects the invader by setting resource availabilities, but the invader does not affect the resident. Evolutionarily stable strategies (ESSs) have asterisks (e.g., R_X^*).

Tree Allometry

All trees share a "toolkit" of organs: leaves to fix carbon, fine roots to capture nutrients and water (either alone or via symbionts), wood to connect and support leaves and fine roots, and reproductive structures. Foresters have successfully described the size of these organs for individuals as functions of stem diameter at breast height (D; e.g., Le Goff and Ottorini 2001; Lambert et al. 2005), and we do as well:

$$\begin{aligned} A(D) &= \pi\alpha^{\theta}D^{\theta}, \\ Q_{\mathrm{X,x}}(D) &= R_{\mathrm{X,x}}\pi\alpha^{\theta}D^{\varphi}, \\ B(D) &= aD^{b}, \\ Z(D) &= hD^{\beta}, \end{aligned} \tag{G1}$$

where $A(D)$ is projected crown area, $Q_{\mathrm{X,x}}(D)$ is living fine root carbon, $B(D)$ is wood carbon, and $Z(D)$ is height. The remaining parameters scale the relationships. A virtue of our approach with respect to projected crown area is that we are not committed to any particular geometry, consistent with the variable crown shapes that canopy trees assume when assembled in a closed canopy. Using forestry data, we show in appendix A that

$$\theta \approx \varphi \approx b - 1. \tag{G2}$$

As in earlier versions of the PPA (Strigul et al. 2008), we assume that fecundity is proportional to $A(D)$ for canopy individuals and 0 for understory individuals.

Nitrogen and Light Availability

The purpose of our model is to understand the community dynamics of nitrogen-limited forests, which play out at timescales of decades to centuries and during which total system nitrogen is approximately constant (Bond-Lamberty et al. 2006), with relatively small inputs balanced by comparable losses (Menge et al. 2009). Consequently, total nitrogen, N_{T}, is effectively conserved within the system:

$$N_{\mathrm{T}} \equiv N_{\mathrm{P}} + N_{\mathrm{M}} + N_{\mathrm{H}} + N_{\mathrm{L}}, \tag{G3}$$

where the nitrogen pools, N, are subscripted for plant (P), soil mineral (M), high-quality organic soil (H), and low-quality organic soil (L).

In the short term, nitrogen availability to plants is determined by the size of the nitrogen pool that is bound to organic molecules (the "organic pool") and the rate at which microbes mineralize that organic pool to plant-available forms (net after microbial immobilization). In addition to temperature and moisture, plant litter quality determines the rate at which microbes can mineralize organic nitrogen. Although the range of plant litter quality forms a continuum from slowly decomposed to quickly decomposed, values of particular compounds across this range are bimodally distributed. Cellulose, lignin, tannins, and materials rich in secondary compounds decompose relatively slowly; amino acids, phenols, and simple carbohydrates decompose relatively quickly (Plante and Parton 2007). It is for this reason that we separate the soil organic pool into N_{L} and N_{H}, with associated decomposition rates d_{L} and d_{H} (Berndt 2008). Moreover, in a nitrogen-limited system, plant uptake of soil mineral nitrogen is orders of magnitude faster (minutes to days) than turnover times in the plant and organic soil pools (months to decades), and thus can be approximated as instantaneous. As a result, the standing pool of mineral nitrogen, N_{M}, is approximately 0 relative to the other pools:

$$N_{\mathrm{T}} \approx N_{\mathrm{P}} + N_{\mathrm{H}} + N_{\mathrm{L}}. \tag{G4}$$

We define the following system, where nitrogen cycles between N_{H} and N_{P} and between N_{L} and N_{P}, and N_{P} loses

nitrogen at rate γ via senescence, mortality, and disturbance, with fraction ψ returning to N_H and fraction $1 - \psi$ returning to N_L:

$$\frac{dN_P}{dt} = d_H N_H + d_L N_L + \gamma N_P, \tag{G5}$$

$$\frac{dN_H}{dt} = -d_H N_H + \psi\gamma N_P, \tag{G6}$$

$$\frac{dN_L}{dt} = -d_L N_L + (1-\psi)\gamma N_P. \tag{G7}$$

It is because we assume that plants take up all mineralized nitrogen that d_H and d_L appear as uptake rates in equation (G5).

At equilibrium,

$$\hat{N}_P = N_T \frac{d_L d_H}{\psi(1-\psi)\gamma^2} \Bigg/ \left[\frac{d_L d_H}{\psi(1-\psi)\gamma^2} + \frac{d_L}{(1-\psi)\gamma} + \frac{d_H}{\psi\gamma}\right], \tag{G8}$$

$$\hat{N}_H = N_T \frac{d_L}{(1-\psi)\gamma} \Bigg/ \left[\frac{d_L d_H}{\psi(1-\psi)\gamma^2} + \frac{d_L}{(1-\psi)\gamma} + \frac{d_H}{\psi\gamma}\right], \tag{G9}$$

$$\hat{N}_L = N_T \frac{d_H}{\psi\gamma} \Bigg/ \left[\frac{d_L d_H}{\psi(1-\psi)\gamma^2} + \frac{d_L}{(1-\psi)\gamma} + \frac{d_H}{\psi\gamma}\right]. \tag{G10}$$

The equations for $\hat{N}_P$, $\hat{N}_H$, and $\hat{N}_L$ describe the concentration of nitrogen residing in each of the three pools at equilibrium and sum to N_T. From a plant's perspective, the equilibrial nitrogen mineralization rate (net after microbial immobilization), N_{avail}, is the sum of the rates from the slow and fast pools:

$$N_{avail} = d_H \hat{N}_H + d_L \hat{N}_L. \tag{G11}$$

Because d_L is smaller than both d_H and γ, and is frequently much smaller (e.g., Alvarez-Sanchez and Enriquez 1996), we can approximate N_{avail} using a Taylor series, expanding N_{avail} around $d_L \approx 0$:

$$N_{avail} \approx \frac{d_L}{1-\psi} N_T. \tag{G12}$$

Here we have derived an approximation of N_{avail} for a monoculture at equilibrium that depends only on total nitrogen in the system, the decomposition rate of low-quality soil organic material, and the fractional composition of litter in terms of high and low quality. The importance of these three terms is based on the fact that a given nitrogen molecule will spend only a relatively brief time in N_P and N_H before returning to N_L for a relatively long time. Thus, d_L directly controls the fate of nitrogen molecules in the very large slow pool itself and indirectly controls the sizes of $\hat{N}_P$ and $\hat{N}_H$ by controlling how much nitrogen is in "circulation" outside of $\hat{N}_L$.

Equation (G12) greatly simplifies our equilibrial forest model without seriously compromising its realism by allowing us to replace a dynamical nitrogen cycling model with just one value. The approximation retains the parts of the cycle that have large effects on the results, while omitting features that greatly complicate the analysis despite their small impacts. The analysis of our model spans a gradient in N_{avail} that, given the physical and physiological constraints on the ranges of possible values for d_L and ψ, is perhaps best thought of as arising from a gradient in N_T. Such gradients abound (Post et al. 1985) and are the legacies of processes at large timescales (Menge et al. 2009).

Light is a directional resource that creates fundamentally different competitive interactions than those of soil resources (Weiner 1990; Dybzinski and Tilman 2007). Taller individuals receive more light than individuals below them. Within an individual, higher leaves receive more light than lower leaves. Our model deals with both the between- and within-individual asymmetries explicitly using Beer's law light extinction through crowns of leaf area index $L_{X,x}$. Note that in contrast to empirical measures of LAI, which are made at the ecosystem level, we define LAI at the individual level as the total one-sided leaf area of an individual divided by its projected

crown area. However, our definition of LAI for canopy individuals will closely accord with empirical measurements in closed-canopy forests where total projected crown area and/or LAI of understory individuals is small.

If I_C^0 is the light intensity at the top of the canopy, $L_{C,r}$ is the uniform canopy LAI in a monoculture, and k is the light extinction coefficient, then the light intensity of a canopy individual's lowest leaves is

$$I_{C,x}^{\text{bottom}} = I_C^0 e^{-kL_{C,x}}, \tag{G13}$$

the light intensity at the top of the understory is

$$I_U^0 = I_C^0 e^{-kL_{C,r}\zeta}, \tag{G14}$$

and the light intensity of an understory individual's lowest leaves is

$$I_{U,x}^{\text{bottom}} = I_U^0 e^{-kL_{U,x}}. \tag{G15}$$

The parameter ζ is between 0 and 1 and scales $L_{C,r}$ and/or k to phenomenologically account for both small-scale disturbance mechanisms (e.g., single tree fall gaps, branch breakage) and wind-driven canopy crown movements (synchronous within individuals but asynchronous among individuals) that can cause understory light intensities to exceed those of the lowest canopy leaves. We include within-individual light extinction in our calculations of photosynthesis in the next section.

Nitrogen and Carbon Capture via Root Competition and Photosynthesis

Root competition is a complex and incompletely understood phenomenon (Schenk 2006). Nevertheless, a few things are clear. The rate-limiting step in nitrogen uptake in most natural systems is diffusion through the soil (Chapin 1980; Raynaud and Leadley 2004; Craine et al. 2005; Lambers et al. 2008), suggesting that despite important differences in root physiology and morphology (Eissenstat 1997; Eissenstat and Yanai 1997), to a first approximation, fine root mass is the greatest determinant of uptake rate and thus competitive ability (Casper and Jackson 1997; Raynaud and Leadley 2004; Lambers et al. 2008). We parameterize fine root mass, $R_{X,x}$, in units of living fine root carbon per crown area, which is positively correlated with the strength of the nitrogen diffusion gradient (Casper and Jackson 1997). We recognize that mycorrhizal associations have the potential to change both nitrogen diffusion gradients and the "exchange rate" of nitrogen acquired per carbon expended, but this important area of ecology is not yet well enough quantified to allow us to incorporate it into our model.

As in earlier models of mean field competition for belowground resources (e.g., Tilman 1988; Reynolds and Pacala 1993; Rees and Bergelson 1997), we assume that the roots of competing plants overlap completely and are uniformly distributed throughout the soil. There are compelling game theoretic reasons to expect plant roots to overlap (e.g., O'Brien et al. 2007), and harvests and tracer studies have demonstrated that the roots of tree species extend well past the drip line (Gilman 1988; Stone and Kalisz 1991; Casper et al. 2003) and are extensively commingled (Gottlicher et al. 2008). We assume that, at minimum, nitrogen-limited plants in closed-canopy forests will possess enough fine root density so that no mineral nitrogen is leached from the system when they are active (i.e., that they can, at minimum, "outcompete gravity"). Consistent with this assumption, studies of unpolluted temperate forests show very low levels of leached mineral nitrogen (e.g., Hedin et al. 1995).

Assuming the same physiology and morphology among strategies (as we do here), the total nitrogen captured by an individual j of stage X and strategy x per unit time, $K_{X,x,j}$, is simply equal to its share (numerator) of the total stand fine root mass (denominator) multiplied by the total amount of nitrogen available per unit time (Berendse and Elberse 1990):

$$K_{X,x,j} = \frac{Q_{X,x,j}(D_j)}{\sum_{i=1}^{n_{C,m}} Q_{C,m}(D_i) + \sum_{i=1}^{n_{C,r}} Q_{C,r}(D_i) + \sum_{i=1}^{n_{U,m}} Q_{U,m}(D_i) + \sum_{i=1}^{n_{U,r}} Q_{U,r}(D_i)} N_{\text{avail}} T, \tag{G16}$$

where D_j is the stem diameter of individual j, T is the total habitat area, i indexes individuals, and $n_{X,x}$ counts individuals. Note that equation (G16) is the result of competition for nitrogen; mineralized nitrogen is divided

among the plants in proportion to their relative fine root mass. Given the allometry of fine root mass (eqq. [G1], [G2]), dividing both sides by crown area yields $N_{\mathrm{X,x}}$, nitrogen uptake on a per crown area basis:

$$N_{\mathrm{X,x}} = \frac{R_{\mathrm{X,x}}}{R_{\mathrm{C,m}} \sum_{i=1}^{n_{\mathrm{C,m}}} A(D_i) + R_{\mathrm{C,r}} \sum_{i=1}^{n_{\mathrm{C,r}}} A(D_i) + R_{\mathrm{U,m}} \sum_{i=1}^{n_{\mathrm{U,m}}} A(D_i) + R_{\mathrm{U,r}} \sum_{i=1}^{n_{\mathrm{U,r}}} A(D_i)} N_{\mathrm{avail}} T, \tag{G17}$$

In anticipation of the adaptive dynamics problems that follow, we assume that strategy r is common and strategy m is rare. This means that

$$\sum_{i=1}^{n_{\mathrm{C,m}}} A(D_i) + \sum_{i=1}^{n_{\mathrm{U,m}}} A(D_i) \ll \sum_{i=1}^{n_{\mathrm{C,r}}} A(D_i) + \sum_{i=1}^{n_{\mathrm{U,r}}} A(D_i). \tag{G18}$$

If we further assume that the sum of the canopy crown areas is equal to the total habitat area (i.e., the canopy is closed),

$$\sum_{i=1}^{n_{\mathrm{C,r}}} A(D_i) \approx T, \tag{G19}$$

and that the total fine root contribution of understory individuals is small relative to the canopy (Le Goff and Ottorini 2001),

$$R_{\mathrm{U,r}} \sum_{i=1}^{n_{\mathrm{U,r}}} A(D_i) \ll R_{\mathrm{C,r}} \sum_{i=1}^{n_{\mathrm{C,r}}} A(D_i), \tag{G20}$$

then nitrogen uptake per projected crown area (eq. [G17]) may be approximated as

$$N_{\mathrm{X,x}} \approx \frac{R_{\mathrm{X,x}}}{R_{\mathrm{C,r}}} N_{\mathrm{avail}}. \tag{G21}$$

Note that equation (G21) can be used to calculate the per crown area nitrogen uptake of either understory or canopy individuals of either the resident or invader strategies by substituting X with either U or C and x with either r or m.

Annual carbon gain of an individual is determined by the light at the top of its crown, the light extinction through its crown, the relationship between light and photosynthesis, and the duration of the growing season. As shown in figure 2 in the main text, we use a simplified model of photosynthesis in which $A_{\max}$ is a leaf's maximum rate of net carbon fixation per area (gross carbon capture minus leaf maintenance respiration) under light saturation, q is the leaf respiration rate, and Φ is the quantum yield. Note that empirically, greater $A_{\max}$ typically comes at the expense of proportionately greater q, though for the sake of generality we do not explicitly model that relationship here. To convert to a yearly timescale, net carbon gain is multiplied by s, which will be positively correlated with growing season length and negatively correlated with factors that decrease annual carbon capture, such as water limitation. Annual net photosynthesis measured on a per crown area basis, $E_{\mathrm{X,x}}$, is the integral of photosynthesis through an individual's crown (i.e., for all layers from the top of the crown to $L_{\mathrm{X,x}}$), assuming Beer's law light extinction due to self-shading, multiplied by s.

There are three distinct cases, depending on whether portions of $L_{\mathrm{X,x}}$ are light saturated, partly light saturated and partly light limited, or solely light limited. The light intensity at which a leaf transitions from light saturated to light limited is $\tilde{I} = (A_{\max} + q)/\Phi$ (fig. 2 in the main text). In case 1, the entire $L_{\mathrm{X,x}}$ is light saturated, such that $I_{\mathrm{X}}^0 > \tilde{I}$ and $I_{\mathrm{X,x}}^{\mathrm{bottom}} \geq \tilde{I}$:

$$E_{\mathrm{X,x}} = s\left(\int_0^{L_{\mathrm{X,x}}} A_{\max} dy\right) = sA_{\max} L_{\mathrm{X,x}}. \tag{G22}$$

In the case 2, part of the $L_{\mathrm{X,x}}$ is light saturated and part is light limited, such that $I_X^0 > \tilde{I}$ and $I_{\mathrm{X,x}}^{\mathrm{bottom}} < \tilde{I}$. Here, we must define and solve for $\tilde{L}_{\mathrm{X}}$, the leaf layer at which light saturation switches to light limitation:

$$\frac{A_{\max} + q}{\Phi} = I_{\mathrm{X}}^0 e^{-k\tilde{L}_{\mathrm{X}}} \Rightarrow \tilde{L}_{\mathrm{X}} = \frac{1}{k} \ln\left(\frac{\Phi I_{\mathrm{X}}^0}{A_{\max} + q}\right). \tag{G23}$$

Its value will be the same for invaders and residents, which is why no x subscript appears. With this, we can calculate $E_{\mathrm{X,x}}$:

$$E_{\mathrm{X,x}} = s\left[\int_0^{\tilde{L}_{\mathrm{X}}} A_{\max}dy + \int_{\tilde{L}_{\mathrm{X}}}^{L_{\mathrm{X,x}}} (\Phi I_{\mathrm{X}}^0 e^{-ky} - q)dy\right]$$

$$= s\left\{\frac{A_{\max}+q}{k}\left[1+\ln\left(\frac{\Phi I_{\mathrm{X}}^0}{A_{\max}+q}\right)\right] - \frac{\Phi I_{\mathrm{X}}^0}{k}e^{-kL_{\mathrm{X,x}}} - qL_{\mathrm{X,x}}\right\}. \quad \text{(G24)}$$

In the third and final case, all of the $L_{\mathrm{X,x}}$ is light limited, such that $I_{\mathrm{X}}^0 < \tilde{I}$:

$$E_{\mathrm{X,x}} = s\left[\int_0^{L_{\mathrm{X,x}}} (\Phi I_{\mathrm{X}}^0 e^{-ky} - q)dy\right] = s\left[\frac{\Phi I_{\mathrm{X}}^0}{k}(1-e^{-kL_{\mathrm{X,x}}}) - qL_{\mathrm{X,x}}\right]. \quad \text{(G25)}$$

We note that in our treatment, we always assume that $I_{\mathrm{C}}^0 > \tilde{I}$, and thus canopy trees are never in case 3. In contrast, because light at the top of understory individuals is reduced by the canopy's shade, understory individuals are often in case 2 or 3.

Nitrogen and Carbon Allocation

Because leaves contain the nitrogen-demanding enzyme rubisco used to fix carbon, nitrogen concentration is clearly related to function (e.g., maximum photosynthetic rate; Evans 1989). Moreover, leaves represent the dominant nitrogen demand in trees and have higher nitrogen concentrations than any other organ (Whittaker et al. 1979; Reich et al. 2008). Trees respond to increased nitrogen primarily through increases in leaf number, and only secondarily through increases in leaf nitrogen concentration (Chapin 1980; Farquhar et al. 2002). The role of nitrogen in fine roots and living wood is less clear; certainly some of the nitrogen is used to maintain basic cell metabolism and ion gradients; some may be used to process compounds for use in the leaves and elsewhere; and some may be in transit. Because diffusion through the soil, not transport across the fine root cell membrane, is the rate-limiting step in nitrogen-limited systems (Chapin 1980; Raynaud and Leadley 2004; Lambers et al. 2008), the total amount of nitrogen used for the transport machinery need not scale with fine root system size and a simple consideration of kinetics would suggest that higher fine root nitrogen concentrations should decrease nitrogen uptake rates per root (Bloom et al. 1985).

For the purposes of this model, we sidestep these important but poorly understood relationships by focusing only on the fraction of total nitrogen uptake that is committed to leaves, with the remainder going to an unspecified black box of fine roots, living wood, reproductive structures, and symbionts. We impose a stoichiometric constraint on an individual's ability to build LAI:

$$L_{\mathrm{X,x}} \le \frac{N_{\mathrm{X,x}}\rho}{\delta_{\mathrm{L}}\gamma_{\mathrm{L}}f}, \quad \text{(G26)}$$

where nitrogen uptake per projected crown area, $N_{\mathrm{X,x}}$, is defined by equation (G21), ρ is the fraction of nitrogen taken up that is allocated to foliage; δ_{L} is the nitrogen concentration of leaves per unit area (although this value is clearly different for sun leaves and shade leaves even within the same individual, we assume for simplicity no change in δ_{L}); f is the fraction of nitrogen lost from senesced foliage; and γ_{L} is leaf turnover.

Fixed carbon is allocated to plant organs and the growth of those organs:

$$\begin{aligned} A(D)E_{\mathrm{X,x}} = {} & A(D)(1+\kappa_{\mathrm{L}})\gamma_{\mathrm{L}}ML_{\mathrm{X,x}} \\ & + A(D)[(1+\kappa_{\mathrm{R}})\gamma_{\mathrm{R}} + \Omega]R_{\mathrm{X,x}} \\ & + \frac{dA(D)}{dt}(1+\kappa_{\mathrm{L}})ML_{\mathrm{X,x}} \\ & + \frac{dA(D)}{dt}(1+\kappa_{\mathrm{R}})R_{\mathrm{X,x}} \\ & + A(D)(1+\kappa_{\mathrm{L}})M\frac{dL_{\mathrm{X,x}}}{dt} \\ & + A(D)(1+\kappa_{\mathrm{R}})\frac{dR_{\mathrm{X,x}}}{dt} \\ & + A(D)\omega_{\mathrm{C}} \\ & + \frac{dB(D)}{dt}, \end{aligned} \tag{G27}$$

where $A(D)$ is projected crown area as a function of stem diameter, $E_{\mathrm{X,x}}$ is the net photosynthetic rate (eqq. [G22], [G24], [G25]), γ_{L} is leaf turnover, M is leaf carbon per one-sided leaf area, κ_{L} is the respiratory cost of building leaves, γ_{R} is fine root turnover, κ_{R} is the respiratory cost of building fine roots, Ω is the maintenance respiration rate of fine roots, ω_{C} is the annual build and maintenance cost of fecundity per projected crown area, and $B(D)$ is wood mass as a function of stem diameter. The equation does not include foliage maintenance respiration, as this is already subsumed in the calculation of net photosynthetic rate. The first two terms on the right-hand side (RHS) describe the carbon costs of existing foliage and fine roots. The third and fourth terms describe the costs incurred by an expanding annulus of new growth. The fifth and sixth terms describe the costs incurred by changing per projected crown area foliage and fine root investments. The seventh term describes the cost of fecundity. The final term describes the change in wood mass, which includes stems, branches, and twigs aboveground and coarse roots of all sizes belowground. We assume negligible wood turnover and respiration.

We show in appendix B that terms associated with a new annulus of growth and changed per crown area $L_{\mathrm{X,x}}$ and $R_{\mathrm{X,x}}$ are small and do not impact the implications of the model. Thus, this conservation equation may be greatly simplified and reordered,

$$\frac{1}{A(D)}\frac{dB(D)}{dt} = E_{\mathrm{X,x}} - (1+\kappa_{\mathrm{L}})\gamma_{\mathrm{L}}ML_{\mathrm{X,x}} - [(1+\kappa_{\mathrm{R}})\gamma_{\mathrm{R}} + \Omega]R_{\mathrm{X,x}} - \omega_{\mathrm{C}}, \tag{G28}$$

to emphasize that carbon allocated to wood increment (left-hand side) is defined by what remains from net photosynthesis (RHS, first term) after allocating to foliage construction (RHS, second term), fine root construction and respiration (RHS, third term), and reproductive structure construction and respiration (RHS, fourth term). Wythers et al. (2005) developed an ecosystem model that allocates carbon in this manner and showed that it accurately predicted both short-term carbon fluxes and long-term forest production of well-measured forests. We can convert equation (G28) into stem diameter growth rate, $G_{\mathrm{X,x}} \equiv dD/dt$, using the allometric equations (eqq. [G1], [G2]):

$$\frac{dB(D)}{dt} = \frac{dB(D)}{dD}\frac{dD}{dt} = (\theta+1)aD^{\theta}\frac{dD}{dt}, \tag{G29}$$

and thus,

$$G_{\mathrm{X,x}} \approx g\{E_{\mathrm{X,x}} - (1+\kappa_{\mathrm{L}})\gamma_{\mathrm{L}}ML_{\mathrm{X,x}} - [(1+\kappa_{\mathrm{R}})\gamma_{\mathrm{R}} + \Omega]R_{\mathrm{X,x}} - \omega_{\mathrm{C}}\}, \tag{G30}$$

where

$$g = \frac{\pi\alpha^{\theta}}{(\theta+1)a}. \tag{G31}$$

Notice that as a consequence of the allometric equations that we use (eqq. [G1], [G2]) and justify in appendix A, stem diameter growth rates $G_{X,x}$ are constant and independent of D, provided that $L_{X,x}$ and I_X^0 are constant. Different strategies will have different $G_{X,x}$ because they have different $L_{X,x}$, $E_{X,x}$, and $R_{X,x}$.

By omitting carbon consumed by respiration, our simplified carbon allocation equation (eq. [G30]) lends itself to comparison with empirical net primary productivity (NPP) measurements:

$$\begin{aligned} \mathrm{NPP}_{\mathrm{foliage}} &\equiv \gamma_L M L_{X,x}, \\ \mathrm{NPP}_{\mathrm{wood}} &\equiv G_{X,x}/g, \\ \mathrm{NPP}_{\mathrm{fine\ root}} &\equiv \gamma_R R_{X,x}, \\ \mathrm{NPP}_{\mathrm{aboveground\ wood}} &= \Lambda \cdot \mathrm{NPP}_{\mathrm{wood}} \\ \mathrm{NPP}_{\mathrm{belowground\ wood}} &= (1-\Lambda) \cdot \mathrm{NPP}_{\mathrm{wood}}, \end{aligned} \tag{G32}$$

where Λ is the fraction of wood allocated aboveground. Note that all five values are expressed in common units ($g_{carbon}\ m^{-2}\ year^{-1}$ for our parameterization; table G1). Relative NPP of any component is found by dividing it by the sum of $\mathrm{NPP}_{\mathrm{foliage}}$, $\mathrm{NPP}_{\mathrm{wood}}$, and $\mathrm{NPP}_{\mathrm{fine\ root}}$.

Stem Growth Rate and the Perfect Plasticity Approximation of Height-Structured Competition

To understand the concept underlying the PPA, it is useful to first consider a forest simulator such as SORTIE (Pacala et al. 1996; Strigul et al. 2008), in which each simulated tree situates its crown symmetrically above its perfectly vertical stem. In SORTIE, the crowns of neighbors may interdigitate, and a tree that is half shaded and half exposed will build leaves equally in both regions. Neither phenomenon is observed in real forests because real trees proliferate branches in empty space, maintain growth toward empty space and away from neighbors, and drop branches that become overtopped (Putz et al. 1984; Purves et al. 2007). As more crown plasticity and phototropism is allowed in a simulator, horizontal canopy space fills more completely (Strigul et al. 2008). The PPA takes this to its asymptotic limit, where the canopy becomes totally filled, with no overlap among the crowns of canopy trees, and the canopy crown join height $\tilde{Z}_r$ is uniform across a stand. With the PPA, it becomes possible to classify individual trees as being in the canopy (as tall as or taller than the minimum canopy crown height $\tilde{Z}_r$) or in the understory (shorter than $\tilde{Z}_r$) without knowing their spatial locations.

The mathematics of the PPA are fully described elsewhere (Adams et al. 2007; Strigul et al. 2008), but we briefly review their essential features here. We note that these previous publications had assumed a value of 2 for θ and do not include it as an explicit parameter. Thus, some formulas appear slightly differently here. The PPA is nonspatial (horizontally) and includes no explicit gaps. In the simplest and analytically tractable version, growth and death rates do not depend on size either in the understory or overstory but do change from understory to overstory. Understory individuals grow stems at rate $G_{U,x}$ and die at rate μ_U. They transition to the canopy when their stems equal $\tilde{D}_r$, the diameter that is allometrically (eq. [G1]) related to $\tilde{Z}_r$ rate $G_{C,x}$, whereupon they die at rate μ_C and produce new understory individuals at rate F per crown area. In a stable-size-distribution (i.e., equilibrial), closed-canopy monoculture, the total canopy crown area is fixed (and equal to the habitat area), and thus the influx of new understory individuals is fixed.

Notice that, in contrast to previous publications (Adams et al. 2007; Strigul et al. 2008), we now explicitly calculate $G_{C,x}$ and $G_{U,x}$ as functions of resource availability, as described in the previous sections. Specifically, given values of $L_{X,x}$ and $R_{X,x}$, one can calculate both $G_{C,x}$ and $G_{U,x}$ using equation (G30), with equations (G22), (G24), or (G25) providing the $E_{X,x}$ term. To be congruent with the simplest version of the PPA, $G_{C,x}$ and $G_{U,x}$ must be constant, which will be true provided individuals maintain their allocational strategies through time and that the allocational shifts between understory and canopy stages are fast relative to the lifetimes of average individuals (and hence negligible). We assume for the moment that allocational strategies are constant for a given stage, but our ESS analysis below reveals that deviations from constant ESSs (for a particular soil nitrogen availability) are less competitive. In appendix B, we show that ignoring the full carbon accounting required to change from $L_{U,x}$ to $L_{C,x}$ and from $R_{U,x}$ to $R_{C,x}$ as individuals transition from the understory stage to the canopy stage has a negligible effect on our calculation of lifetime reproductive success. Thus, our model of individual

trees competing for light and nitrogen generates constant $G_{U,x}$ and constant $G_{C,x}$, consistent with the analytically tractable version of the PPA as described in Strigul et al. (2008).

With the PPA, we calculate an individual's expected lifetime reproductive success (or fitness, W_x) by summing its total fecundity over its lifetime. To do this for an average individual, we must calculate the average fraction of understory individuals that will survive to the canopy, assuming their initial diameter is negligible:

$$\exp\left(-\frac{\mu_U}{G_{U,x}}\tilde{D}_r\right) \tag{G33}$$

where $\tilde{D}_r$ is the diameter of strategy r individuals at the transition from understory to canopy (the diameter corresponding to height $\tilde{Z}_r$; eq. [G1]). The fraction of individuals that entered the canopy and then survived for τ years is

$$\exp(-\mu_C\tau), \tag{G34}$$

and the fecundity of an individual that has survived τ years in the canopy is

$$FA(D) = F\pi\alpha^\theta(\tilde{D}_r + G_{C,x}\tau)^\theta. \tag{G35}$$

Combining these three equations, we integrate over all time to calculate fitness:

$$W_x = \exp\left(-\frac{\mu_U}{G_{U,x}}\tilde{D}_r\right)\int_0^\infty \exp(-\mu_C\tau)F\pi\alpha^\theta(\tilde{D}_r + G_{C,x}\tau)^\theta d\tau. \tag{G36}$$

By changing variables twice, the solution is an incomplete gamma, which we can reasonably approximate as a complete gamma:

$$W_x \approx F\pi\alpha^\theta\Gamma(\theta+1)\frac{G_{C,x}^\theta}{\mu_C^{\theta+1}}\exp\left[-\left(\frac{\mu_U}{G_{U,x}} - \frac{\mu_C}{G_{C,x}}\right)\tilde{D}_r\right], \tag{G37}$$

where $\Gamma(\ldots)$ represents the gamma function. The equation for W_x embodies the combined effects of interspecific (or interstrategic) competition for both nitrogen and light through its effects on both the canopy and understory stages of residents and invaders. The resident influences itself and the invader through its effects on nitrogen competition, light availability in the understory, and, by setting $\tilde{D}_r$, the length of time that individuals spend in the understory.

At equilibrium, each individual exactly replaces itself over its lifetime, that is, $W_r = 1$, and we are able to solve for $\tilde{D}_r$ in a monoculture:

$$\tilde{D}_r \approx \left(\frac{\mu_U}{G_{U,r}} - \frac{\mu_C}{G_{C,r}}\right)^{-1}\ln\left[F\pi\alpha^\theta\Gamma(\theta+1)\frac{G_{C,r}^\theta}{\mu_C^{\theta+1}}\right]. \tag{G38}$$

For closed-canopy forests, $\tilde{D}_r$ is always greater than or equal to 0. When this condition is not true, the canopy will open, and a different set of tools and assumptions are needed to evaluate dynamics. Here, we restrict our analysis to allocation strategies that are capable of sustaining closed-canopy conditions in monoculture.

Because $\mu_U > \mu_C$ and $G_{U,x} \le G_{C,x}$, it will frequently be the case that $\mu_U/G_{U,x} \gg \mu_C/G_{C,x}$ and thus that

$$\tilde{D}_r \approx \frac{G_{U,r}}{\mu_U}\ln\left[F\pi\alpha^\theta\Gamma(\theta+1)\frac{G_{C,r}^\theta}{\mu_C^{\theta+1}}\right] \tag{G39}$$

and

$$W_x \approx F\pi\alpha^\theta\Gamma(\theta+1)\frac{G_{C,x}^\theta}{\mu_C^{\theta+1}}\exp\left(-\tilde{D}_r\frac{\mu_U}{G_{U,x}}\right). \tag{G40}$$

For numerical work, we use the more complete expressions (eqq. [G37], [G38]). For analytical work we use the simplified expressions (eqq. [G39], [G40]).

Determining Evolutionary Stable Strategies

We analyze our model to determine the change in ESS allocations to foliage, wood, and fine roots with N_{avail}. We can use the equation for the fitness of a rare invader W_{m} in the equilibrium conditions created by a resident r (eq. [G40]) to find the ESS, if it exists. See Strigul et al. (2008) for a proof that an equilibrial monoculture of the PPA model is locally stable for reasonable parameter values, as is required of this analysis. By definition, the expected W_{r} of a resident individual in an equilibrial monoculture is 1; that is, it will exactly replace itself in its lifetime. Consistent with the assumptions of standard adaptive dynamics analyses (McGill and Brown 2007), we model a stand of infinite size and an invasion process of potentially infinite duration, such that any invader with W_{m} greater than 1 will successfully invade the resident. We use the term ESS to describe a strategy that, once established as a monoculture, cannot be invaded by any rare mutant strategy (McGill and Brown 2007). In other words, the ESS is a strategy r for which no W_{m} is greater than 1.

For a particular trait v, we find the ESS, v^*, by finding the maxima of W_{m} for v:

$$\left.\frac{dW_{\text{m}}(v_{\text{m}}, v_{\text{r}})}{dv_{\text{m}}}\right|_{v_{\text{m}}=v_{\text{r}},\, v_{\text{r}}=v^*} = 0,$$

$$\left.\frac{dW_{\text{m}}^2(v_{\text{m}}, v_{\text{r}})}{d^2 v_{\text{m}}}\right|_{v_{\text{m}}=v_{\text{r}},\, v_{\text{r}}=v^*} < 0, \tag{G41}$$

where W_{m} is a function of both the invader's strategy v_{m} and the resident's strategy v_{r} and is both continuous and smooth within the domain of analysis. Because of their functional connection to $G_{\text{X, x}}$ (eq. [G30]), solutions for L_{X}^* and R_{X}^* uniquely determine G_{X}^*. We determine that the ESS values that we find are both global and convergence stable in appendix F.

Derivation of Theoretical Results

Result 1

Increasing ESS foliage with increasing nitrogen availability. Across a fertility gradient, as N_{avail} increases, the most competitive LAI in both the canopy L_{C}^* and the understory L_{U}^* increase up to the point of nitrogen saturation (fig. 3). The canopy light environment is unaffected by $L_{\text{U, r}}^*$, but the reverse is not true, so we begin by solving for L_{C}^*. We solve the ESS condition (eq. [G41]) using the growth rate equation (eq. [G30]) together with either light-saturated or dual-limited net photosynthesis (eqq. [G22], [G24]), assuming for the moment unlimited nitrogen availability to build foliage:

$$L_{\text{C}}^{*\text{sat}} = \frac{1}{k}\ln\left[\frac{s\Phi I_{\text{C}}^0}{(1+\kappa_{\text{L}})\gamma_{\text{L}}M + sq}\right], \tag{G42}$$

where "sat" indicates that this is the nitrogen-saturated result. Interpretation of this equation is straightforward. The $L_{\text{C}}^{*\text{sat}}$ depends strongly on k, the light extinction coefficient; smaller k leads to greater $L_{\text{C}}^{*\text{sat}}$ because it decreases self-shading. Of those variables that may vary appreciably among species or habitats, increased $L_{\text{C}}^{*\text{sat}}$ occurs with increasing extrapolated net photosynthetic rate s or decreasing leaf turnover rate γ_{L}, leaf carbon per area M, or leaf dark respiration rate q. Because A_{max} and q are often positively correlated, decreasing A_{max} will likely increase $L_{\text{C}}^{*\text{sat}}$. At $L_{\text{C}}^{*\text{sat}}$, the lowest leaves of canopy trees are just able to pay for their own construction and respiratory costs. This is an upper limit, as it does not take into account the possibility that additional whole-plant respiratory costs are required to support those lowest leaves (Reich et al. 2009).

It is easy to show that in habitats with less than saturating nitrogen availability (i.e., $N_{\text{C, r}}\rho/\delta_{\text{L}}\gamma_{\text{L}}f < L_{\text{C}}^{*\text{sat}}$; eq. [G26]), a strategy that builds as much foliage as it can (i.e., $N_{\text{C, r}}\rho/\delta_{\text{L}}\gamma_{\text{L}}f$) will invade a strategy that builds $L_{\text{C, r}}$ less than that (see "Result 5"). Thus,

$$L_{\text{C}}^* = \min\left(\frac{N_{\text{avail}}\rho}{\delta_{\text{L}}\gamma_{\text{L}}f}, L_{\text{C}}^{*\text{sat}}\right), \tag{G43}$$

where $N_{C,r}$ has been replaced (eq. [G21]; $m = r$ at the ESS) and L_C^{*sat} is defined by equation (G42).

Having calculated L_C^* and thus I_U^0 (via eq. [G14]) in a monoculture composed of competitively dominant canopy individuals, we are now in a position to determine L_U^*. In an analysis that parallels that of the canopy, we find

$$L_U^{*sat} = \frac{1}{k}\ln\left[\frac{s\Phi I_U^0}{(1+\kappa_L)\gamma_L M + sq}\right] \tag{G44}$$

and

$$L_U^* = \min\left(\frac{N_{avail}\rho}{\delta_L\gamma_L f}\frac{R_U^*}{R_C^*}, L_U^{*sat}\right). \tag{G45}$$

After solving for R_U^* below (eq. [G47]) and substituting, one can show that the nitrogen-limited form of L_U^* is monotonically increasing with L_C^*/R_C^* and thus with N_{avail}.

These results show that the most competitive L_X^* strategy is that which builds as much foliage as it has nitrogen for, up to the point at which additional leaves would fail to pay for themselves due to self-shading. This result provides constant $G_{C,x}$ and $G_{U,x}$ as assumed in the simple version of the PPA used here.

Result 2

Decreasing ESS fine root mass with increasing nitrogen availability. Across a soil fertility gradient as N_{avail} increases, the most competitive fine root mass R_X^* decreases monotonically. No closed-canopy R_X^* exists at low N_{avail} because successful invaders with greater $R_{C,m}$ drive the system into open-canopy, nonforest conditions (see app. C). For all N_{avail} sufficiently large, a stable R_X^* exists up to the point at which the canopy becomes nitrogen saturated (fig. 3).

The effects of $R_{U,r}$ on the canopy nitrogen environment are negligible, but the reverse is not true, so we begin by solving for R_C^*. We solve the ESS condition (eq. [G41]) using the simplified carbon conservation equation (eq. [G30]) together with $E_{C,m}$ case 2 (eq. [G24]; in app. C we show that no R_C^* exists for $E_{C,m}$ case 1):

$$R_C^* = \frac{s\Phi I_C^0 e^{-kL_C^*} - sq - (1+\kappa_L)\gamma_L M}{(1+\kappa_R)\gamma_R + \Omega}L_C^*. \tag{G46}$$

For reasonable parameter values, R_C^* decreases with N_{avail} for all values of R_C^* that generate closed-canopy forest (L_C^* is an increasing function of N_{avail}; eq. [G43]). Root mass R_C^* is both a global ESS and convergent stable (app. F). It is easy to show that R_C^* goes to 0 as L_C^* goes to L_C^{*sat} (eq. [G42]), demonstrating that the premium paid on fine root biomass for the purpose of nitrogen uptake goes to 0 as nitrogen becomes nonlimiting (assuming, as we do, no leaching of nitrogen).

Equation (G46) is a ratio. The quantum yield, Φ, is the slope of light-limited photosynthesis with light availability (fig. 2), and $I_C^0\exp(-kL_C^*)$ is light availability at the lowest leaf layer. Thus, the first term in the numerator describes the rate of light-limited photosynthesis at the lowest leaf layer. The second and third terms in the numerator are the respiratory and build costs of that leaf layer. Together, the numerator is the net marginal carbon benefit given to an invader with greater fine root mass than the resident. Whenever an individual is at least partially light limited, this marginal benefit will decrease with N_{avail} because L_C^* increases and thus the light at the bottom of the canopy due to self-shading will decrease. The denominator for R_C^* is the fixed carbon cost of that infinitesimally greater root investment. In contrast to the numerator, this fixed root cost never varies with N_{avail}. Simply put, R_C^* decreases with N_{avail} because the marginal benefit to greater root investment decreases while the cost remains fixed.

By reasonable approximation, resident understory individuals will have a negligible effect on the light environment and nitrogen availability for resident canopy individuals or invaders. We need not consider the case of a light-saturated understory, $E_{U,r}$ case 1 (eq. [G22]), because no R_C^* exists for closed-canopy, light-saturated

conditions. The answers for a partially light-limited understory, $E_{\mathrm{U,r}}$ case 2 (eq. [G24]), or totally light-limited understory, $E_{\mathrm{U,r}}$ case 3 (eq. [G25]), are the same:

$$R_{\mathrm{U}}^{*} = \frac{1}{k}\frac{R_{\mathrm{C}}^{*}}{L_{\mathrm{C}}^{*}}\ln\left\{\frac{s\Phi I_{\mathrm{U}}^{0}L_{\mathrm{C}}^{*}}{[sq + (1+\kappa_{\mathrm{L}})\gamma_{\mathrm{L}}M]L_{\mathrm{C}}^{*} + [(1+\kappa_{\mathrm{R}})\gamma_{\mathrm{R}} + \Omega]R_{\mathrm{C}}^{*}}\right\}. \tag{G47}$$

Root mass R_{U}^{*} is most sensitive to the variables outside the natural log, which reflect the dominant nitrogen (R_{C}^{*}) and light environments (L_{C}^{*}). It is both a global ESS and convergent stable (app. F).

Result 3

Increasing ESS growth rates with increasing nitrogen availability. The most competitive growth rate in the canopy, G_{C}^{*}, increases monotonically and saturates with increasing N_{avail}. Having solved for L_{C}^{*} (eq. [G43]) and R_{C}^{*} (eq. [G46]), we need only substitute them into the carbon balance equation (eq. [G30]) to determine G_{C}^{*}:

$$G_{\mathrm{C}}^{*} = \frac{\pi\alpha^{\theta}}{(\theta+1)a}\left\{\frac{(A_{\max}+q)s}{k}\left[1 + \ln\left(\frac{\Phi I_{\mathrm{C}}^{0}}{A_{\max}+q}\right)\right] - (kL_{\mathrm{C}}^{*}+1)\frac{s\Phi I_{\mathrm{C}}^{0}}{k}e^{-kL_{\mathrm{C}}^{*}} - \omega_{\mathrm{C}}\right\}. \tag{G48}$$

Over the range of N_{avail} for which the model predicts closed-canopy forest, the term involving the exponent becomes less negative with increasing N_{avail}, causing the whole function to increase but in a saturating way. Apart from the conversion constants in front and the cost of fecundity, equation (G48) differs from the equation for net photosynthesis (eq. [G24]) by the addition of kL_{C}^{*} to the term involving the exponent, which effectively incorporates the increasing cost of L_{C}^{*} and the decreasing cost of R_{C}^{*} with N_{avail}.

It is also possible to solve analytically for G_{U}^{*} by a similar substitution. However, the resulting expression is neither simple nor illuminating. We omit it here.

Result 4

Forests composed of individuals with ESSs are dual limited up to the point of nitrogen saturation. Up to the point of nitrogen saturation, where no tree in a stand is limited by nitrogen, our model predicts that all ESS forests are dual limited; that is, the canopy, and sometimes the understory, is limited by both nitrogen and light. At low N_{avail}, where both the canopy and understory would be solely nitrogen limited, no ESS closed-canopy forest can exist because strategies that lead to open-canopy conditions always successfully invade (app. C). Only after the canopy becomes dual limited with increasing N_{avail} does the possibility exist for an ESS closed-canopy forest. As N_{avail} increases, the understory transitions from dual limited to solely light limited. At the point of nitrogen saturation, no individual is limited by nitrogen and both the understory and canopy are at $L_{\mathrm{X}}^{*\mathrm{sat}}$ (eqq. [G42], [G44]).

Result 5

Under nitrogen-limited conditions, ESS foliage maximizes competitive ability and stem growth rate in monoculture (*i.e., is "optimal"*)*, whereas ESS fine root mass and wood allocation maximize only competitive ability* (*i.e., are not "optimal"*). By design, our method for determining ESSs (eq. [G41]) finds those strategies that are uninvadible and thus the most competitive among all neighboring strategies. In much of the literature on plant ecology, plants are assumed to maximize carbon gain or individual growth rate in monoculture, that is, are said to be "optimal." In addition to being the most competitive strategy, ESS foliage L_{C}^{*} is optimal in this sense, but ESS fine root mass R_{C}^{*} and growth rate G_{C}^{*} are not. This can be seen by asking whether any perturbation, ε, of the ESS leads to greater growth rate of the resident, $G_{\mathrm{C,r}}$. If it does, the strategy is not optimal in this sense.

Under nitrogen-limited conditions, plants use all of the nitrogen they acquire with a particular $R_{\mathrm{C,m}}$ to build $L_{\mathrm{C,m}}$ (eqq. [G43], [G45]), so the only stoichiometrically possible perturbation in $L_{\mathrm{C,m}}$ itself (independent of $R_{\mathrm{C,m}}$) is a decrease (see inequality in eq. [G26]). Using equations (G24) and (G30) to calculate $G_{\mathrm{C,m}}$ (eq. [G30]) with the perturbation term $L_{\mathrm{C}}^{*}(1-\varepsilon)$ and a Taylor series expanding the result around $\varepsilon \sim 0$, we find the change in the resident growth rate, $\Delta G_{\mathrm{C,r}}$, for a perturbation that decreases $L_{\mathrm{C,r}}$:

$$\Delta G_{\mathrm{C,r}} = [-s\Phi I_{\mathrm{C}}^{0}e^{-kL_{\mathrm{C}}^{*}} + sq + (1+\kappa_{\mathrm{L}})\gamma_{\mathrm{L}}M]L_{\mathrm{C}}^{*}. \tag{G49}$$

This will be negative provided $L_{\mathrm{C}}^{*} < L_{\mathrm{C}}^{*\mathrm{sat}}$, which is true here by assumption.

Under nitrogen-saturated conditions, plants can build $L_{C,m}$ greater than L_C^{*sat}. A parallel analysis to that above shows that a perturbation of increased $L_{C,m}$ under nitrogen-saturated conditions leads to lower growth rates provided $L_C^* = L_C^{*sat}$, which is true here by assumption. Taking the nitrogen-limited and nitrogen-saturated results together, it follows that L_C^* maximizes growth rates in monoculture, that is, is "optimal."

In contrast, any perturbation that reduces R_C^*, that is, $R_C^*(1 - \varepsilon)$, invariably leaves more carbon to allocate to wood and thus increases $\Delta G_{C,r}$:

$$\Delta G_{C,r} = (1 + \kappa_R)\gamma_R R_C^* + \Omega R_C^* > 0. \tag{G50}$$

Thus, R_C^* and G_C^* (via its functional relationship with R_C^*) do not maximize growth rates in monoculture, that is, are not "optimal."

Table G1. Traits subject to evolutionarily stable strategy analysis: model parameters and subscripts

Symbol	Value	Units	Description
$L_{X,x}$	Any	$m^2\ m^{-2}$	Leaf area index; one-sided area of leaves per ground surface area of an individual, proportional to carbon allocation to foliage
$G_{X,x}$	Any	cm $year^{-1}$	Stem diameter growth rate, proportional to carbon allocation to wood
$R_{X,x}$	Any	$g_{carbon}\ m^{-2}$	Live fine root mass per crown area; coefficient relating D to $R_{X,x}$, proportional to carbon allocation to fine roots
Allometric relationships:			
D	Any	cm	Stem diameter
A	Any	m^2	Individual tree crown area (projected)
α	.1	$m^{2/\theta}\ cm^{-1}$	Power law coefficient relating D to A
θ	1.4	None	Power law coefficient relating D to A
$Q_{X,x}$	Any	g_{carbon}	Individual tree fine root mass
φ	1.4	None	Power law exponent relating D to $R_{X,x}$
B	Any	g_{carbon}	Individual tree mass
a	81.5	$g_{carbon}\ cm^{-(\theta+1)}$	Power law coefficient relating D to B
b	2.4	None	Power law exponent relating D to B
Z	Any	m	Individual tree height
h	3.58	$m\ cm^{-\beta}$	Power law coefficient relating D to H
β	.5	None	Power law exponent relating D to H
Nitrogen:			
T	Any	m^2	Total habitat area
N_T, N_M, N_P, N_H, N_L	Any	$g_N\ m^{-2}$	Nitrogen pools: total habitat, soil mineral, plant, high-quality soil organic, low-quality soil organic, respectively
γ	...	$year^{-1}$	Whole-plant nitrogen loss rate
d_H, d_L	...	$year^{-1}$	High- and low-quality soil organic decomposition rates, respectively
ψ	0–1	Fraction	Fraction of plant nitrogen that goes to the high-quality soil organic pool
N_{avail}	Any	$g_N\ m^{-2}\ year^{-1}$	Available nitrogen per area
$K_{X,x}$	Any	g_N	Total nitrogen uptake of an individual
$N_{X,x}$	Any	$g_N\ m^{-2}$	Nitrogen uptake of an individual per crown area
ρ	.5	None	Fraction of total plant nitrogen uptake allocated to leaves
δ_L	1.595	$g_N\ m^{-2}$	Nitrogen per unit leaf area
f	.5	None	Fraction of nitrogen lost from senesced foliage
γ_L	1	$year^{-1}$	Foliage turnover
Light and photosynthesis:			
I_X^0	0–1	PAR PAR_0^{-1}	Light level of the highest leaf layer
$I_{X,x}^{bottom}$	0–1	PAR PAR_0^{-1}	Light level of the lowest leaf layer
$\tilde{I}$	.33	PAR PAR_0^{-1}	Light level at which photosynthesis is balanced between light limited and light saturated; equal to $(A_{max} + q)/\phi$
A_{max}	9.9×10^{-5}	$g_{carbon}\ LAI^{-1}\ m^{-2}\ s^{-1}$	Maximum net carbon assimilation rate (see fig. 2)
q	9.9×10^{-6}	$g_{carbon}\ LAI^{-1}\ m^{-2}\ s^{-1}$	Dark respiration rate (see fig. 2)
Φ	3.27×10^{-4}	$g_{carbon}\ LAI^{-1}\ m^{-2}\ s^{-1}\ PAR^{-1}\ PAR_0$	Quantum yield of light-limited net photosynthesis (see fig. 2)
s	2.26×10^6	s $year^{-1}$	Scale conversion between measured (s^{-1}) and yearly net photosynthesis
k	.5	LAI^{-1}	Light extinction coefficient per crown depth
ζ	.75	None	Scales k and $LAI_{C,r}$ in Beer's law light extinction to calculate I_U^0
$\tilde{L}_X$	Any	LAI	Crown depth at which photosynthesis transitions from light saturated to light limited

Table G1 (*Continued*)

Symbol	Value	Units	Description
Carbon:			
$E_{X,x}$	Any	$g_{carbon}\ m^{-2}\ year^{-1}$	Carbon fixed per projected crown area, net after leaf maintenance respiration
M	28	$g_{carbon}\ LAI^{-1}\ m^{-2}$	Leaf carbon per area
κ_L	.25	None	Foliage construction respiration, expressed as a fraction of leaf carbon
γ_R	.3	$year^{-1}$	Fine root turnover
κ_R	.25	None	Fine root construction respiration, expressed as a fraction of fine root carbon
Ω	.35	$g_{carbon}\ g_{carbon}^{-1}\ year^{-1}$	Fine root respiration rate
ω_C	34.6, 0	$g_{carbon}\ m^{-2}\ year^{-1}$	Carbon cost of producing seeds; 0 for understory individuals
g	$8.14E^{-4}$	$cm\ (g_{carbon}/m^2)^{-1}$	Scale conversion between net carbon per canopy area and diameter growth rate (eq. [G31])
Λ	.78	None	Fraction aboveground of the carbon allocated to wood
Perfect plasticity approximation:			
W_x	Any	individuals	Fitness or lifetime reproductive success of strategy x
D_r^*	Any	cm	Stem diameter of shortest cohort in the canopy of a monoculture
Z_r^*	Any	m	Height of shortest cohort in the canopy of a monoculture as determined from height allometry (eq. [G1])
τ	Any	year	Years spent in the canopy stage
μ_X	.013, .038	$year^{-1}$	Mortality rate for canopy and understory, respectively
F	.01	individuals $m^{-2}\ year^{-1}$	Germinants produced per unit canopy area per time

Note: Sources and derivations for values are in appendix E. Subscripts and superscripts: r = variables for resident strategies; m = variables for invading strategies; x = a "placeholder" for variables that can take either an r or an m; C = variables for canopy individuals; U = variables for understory individuals; X = a "placeholder" for variables that can take either C or U; asterisk = variables for evolutionarily stable strategies; sat = variables calculated assuming saturating nitrogen uptake. PAR = photosynthetically active radiation; LAI = leaf area per ground area of an individual.

Additional Literature Cited in Appendix G

Alvarez-Sanchez, J., and R. B. Enriquez. 1996. Leaf decomposition in a Mexican tropical rain forest. Biotropica 28:657–667.

Berendse, F., and W. T. Elberse. 1990. Competition and nutrient availability. Pages 93–115 *in* J. B. Grace and D. Tilman, eds. Perspectives on plant competition. Academic Press, San Diego, CA.

Berndt, W. L. 2008. Double exponential model describes decay of hybrid Bermudagrass thatch. Crop Science 48: 2437–2446.

Bloom, A. J., F. S. Chapin, and H. A. Mooney. 1985. Resource limitation in plants: an economic analogy. Annual Review of Ecology and Systematics 16:363–392.

Bond-Lamberty, B., S. T. Gower, C. Wang, P. Cyr, and H. Veldhuis. 2006. Nitrogen dynamics of a boreal black spruce wildfire chronosequence. Biogeochemistry 81:1–16.

Casper, B. B., and R. B. Jackson. 1997. Plant competition underground. Annual Review of Ecology and Systematics 28:545–570.

Chapin, F. S., III. 1980. The mineral nutrition of wild plants. Annual Review of Ecology and Systematics 11:233–260.

Craine, J. M., J. Fargione, and S. Sugita. 2005. Supply pre-emption, not concentration reduction, is the mechanism of competition for nutrients. New Phytologist 166:933–940.

Dybzinski, R., and D. Tilman. 2007. Resource use patterns predict long-term outcomes of plant competition for nutrients and light. American Naturalist 170:305–318.

Eissenstat, D. 1997. Trade-offs in root form and function. Pages 173–199 *in* L. E. Jackson, ed. Ecology in agriculture. Academic Press, San Diego, CA.

Eissenstat, D. M., and R. D. Yanai. 1997. The ecology of root lifespan. Advances in Ecological Research 27:1–60.

Evans, J. R. 1989. Photosynthesis and nitrogen relationships in leaves of C_3 plants. Oecologia (Berlin) 78:9–19.

Farquhar, G. D., T. N. Buckley, and J. M. Miller. 2002. Optimal stomatal control in relation to leaf area and nitrogen content. Silva Fennica 36:625–637.

Harpole, W. S., and L. Goldstein. 2007. Resource limitation. Pages 119–127 *in* M. Stromberg, J. Corbin, and C. D'Antonio, eds. California grasslands: ecology and management. University of California Press, Berkeley.

Hedin, L. O., J. J. Armesto, and A. H. Johanson. 1995. Patterns of nutrient loss from unpolluted, old-growth temperate forests: evaluation of biogeochemical theory. Ecology 76:493–509.

Lambers, H., F. S. Chapin, and T. L. Pons. 2008. Plant physiological ecology. Springer, New York..

Lambert, M. C., C. H. Ung, and F. Raulier. 2005. Canadian national tree aboveground biomass equations. Canadian Journal of Forest Research 35:1996–2018.

Le Goff, N., and J. M. Ottorini. 2001. Root biomass and biomass increment in a beech (*Fagus sylvatica* L.) stand in north-east France. Annals of Forest Science 58:1–13.

Menge, D. N. L., S. W. Pacala, and L. O. Hedin. 2009. Emergence and maintenance of nutrient limitation over multiple timescales in terrestrial ecosystems. American Naturalist 173:164–175.

Plante, A. F., and W. J. Parton. 2007. The dynamics of soil organic matter and nutrient cycling. Pages 433–470 *in* E. A. Paul, ed. Soil microbiology, ecology, and biochemistry. Academic Press, New York.

Post, W. M., J. Pastor, P. J. Zinke, and A. G. Stangenberger. 1985. Global patterns of soil nitrogen storage. Nature 317:613–616.

Reich, P. B., M. G. Tjoelker, K. S. Pregitzer, I. J. Wright, J. Oleksyn, and J. L. Machado. 2008. Scaling of respiration to nitrogen in leaves, stems and roots of higher land plants. Ecology Letters 11:793–801.

Schenk, H. J. 2006. Root competition: beyond resource depletion. Journal of Ecology 94:725–739.

Stone, E. L., and P. J. Kalisz. 1991. On the maximum extent of tree roots. Forest Ecology and Management 46: 59–102.

Weiner, J. 1990. Asymmetric competition in plant populations. Trends in Ecology & Evolution 5:360–364.

Whittaker, R. H., G. E. Likens, F. H. Bormann, J. S. Easton, and T. G. Siccama. 1979. The Hubbard Brook ecosystem study: forest nutrient cycling and element behavior. Ecology 60:203–220.

Wythers, K. R., P. B. Reich, M. G. Tjoelker, and P. B. Bolstad. 2005. Foliar respiration acclimation to temperature and temperature variable Q_{10} alter ecosystem carbon balance. Global Change Biology 11:435–449.